Supplementary Materials for

MORC family ATPases required for heterochromatin condensation and gene silencing

Guillaume Moissiard[1], Shawn J. Cokus[1], Joshua Cary[1], Suhua Feng[1], Allison C. Billi[2], Hume Stroud[1], Dylan Husmann[1], Ye Zhan[3], Bryan R. Lajoie[3], Rachel P. McCord[3], Christopher J. Hale[1], Wei Feng[4], Scott D. Michaels[4], Alison R. Frand[5], Matteo Pellegrini[1,6], Job Dekker[3], John K. Kim[2], and Steve Jacobsen[1,5,6,7] *

[1]Department of Molecular, Cell, and Developmental Biology, University of California at Los Angeles, Terasaki Life Sciences Building, 610 Charles Young Drive East, Los Angeles, California 90095-723905, USA.

[2]Life Sciences Institute and Department of Human Genetics, University of Michigan, Ann Arbor, Michigan, USA.

[3]Lazare Research Building 570N, Program in Systems Biology and Gene Function and Expression, University of Massachusetts Medical School, 364 Plantation Street, Worcester, MA, 01605, USA

[4]Department of Biology, Indiana University, Bloomington, Indiana, USA.

[5]Department of Biological Chemistry, David Geffen School of Medicine, University of California Los Angeles, Los Angeles, California, USA.

[6]Eli & Edythe Broad Center of Regenerative Medicine & Stem Cell Research, University of California Los Angeles, Los Angeles, California, USA.

[7]Howard Hughes Medical Institute, University of California Los Angeles, Los Angeles, California, USA.

*Correspondence to: jacobsen@ucla.edu

Material and Methods:

Plant material and growing conditions.

All mutants are in the Columbia (Col) ecotype. *atmorc6-3* (GK_599B06) and *atmorc1-4* (SAIL_1239_C08) T-DNA lines were obtained from GABI-Kat (*24*) at University of Bielefeld, Germany and ABRC at Ohio State University, respectively. *drm2-2* (SALK_150863.37.35) and *cmt3-11* (SALK_148381) were previously described (*4*). T-DNA insertions were confirmed by PCR-based genotyping. Primer sequences are described in Table S4. *Arabidopsis* plants were grown under continuous light.

Cloning of *SDC::GFP*.

NLS-GFP-35S terminator was PCR amplified and cloned into pCambia3300. The *SDC* promoter corresponding to a region of ~2.4 kb upstream of *SDC* transcriptional start site was PCR amplified from wild type genomic DNA and cloned into pCR2.1 TOPO vector (Invitrogen). Quick change site-directed mutagenesis (Stratagene) was performed to create a polymorphism (NlaIII -> BamHI) within the *SDC* promoter, which was subsequently mobilized into pCambia3300 upstream of NLS-GFP sequence. *drm2 cmt3* double mutant plants were transformed with the *SDC::GFP* construct using the *Agrobacterium*-mediated floral dip method (*25*). Transgenic plants showing strong GFP fluorescence were backcrossed with a wild type plant to ensure proper silencing of *SDC::GFP* in the F_1 generation. F_1 plants were self-crossed and their progenies (F_2) were screened for GFP fluorescence and PCR-based genotyped to obtained the following genetic backgrounds: *SDC::GFP* wt, *SDC::GFP drm2, SDC::GFP cmt3* and *SDC::GFP drm2 cmt3*. Primer sequences used for *SDC::GFP* cloning are described in Table S4.

Cloning of *pAtMORC1::AtMORC1-Myc* and *pAtMORC6::AtMORC6-Myc*.

AtMORC1 and *AtMORC6* genomic regions were PCR amplified and the Myc epitope was added to the C-terminus of each protein as previously described (*26*). In both cases, the amplified region includes a ~1Kb promoter sequence upstream of the respective transcriptional start site. Primer sequences are described in Table S4.

EMS mutagenesis, GFP screening and mapping analyses.

Two thousand seeds from *SDC::GFP* wt and *SDC::GFP cmt3* lines were mutagenized in 0.3% EMS solution for 13 hours with rotation. Seeds were subsequently washed with water and planted onto soil. For each background, approximately one thousand M2 populations were collected and subsequently screened for GFP fluorescence under UV light using a Leica MZ16F Fluorescence Stereomicroscope coupled with the GPF Plus fluorescence filter. Pictures were taken using the DFC300 FX digital camera kit. Mapping and identification of the three EMS mutations responsible for the phenotypes were performed by bulk segregant analysis coupled with deep genome re-sequencing as previously described (*27*), using single nucleotide polymorphisms (SNPs) between the Landsberg (L*er*) and Col ecotypes derived *de novo* from data from a large number of mapping crosses.

Western Blotting.

Western blots against GFP were performed using the GFP-specific antibody (Invitrogen, AA1122). Western blots against Myc were performed as previously described (*26*).

RNA analyses.

Total RNAs were extracted from two-week-old seedlings using Trizol (Ambion RNA technology). Two µg of total RNAs were subsequently used to generate libraries for High Throughput RNA sequencing (TruSeq RNA, Illumina) per manufacturer instruction. For RNA-seq analyses, sequencing reads were mapped with Bowtie (*28*) allowing up to 2 mismatches. Gene and transposon expression was measured by calculating reads per kilobase per million mapped reads (RPKM) (*29*). *p*-values were calculated using Fisher's exact test and Benjamini corrected for multiple testing (*30*). Differentially expressed elements in wild type and mutants were defined by applying $\log_2$(*mutant* /wild type)>2 and P<0.05 cutoffs. For quantitative PCR analysis, total RNAs were converted into cDNA using SuperScript III Reverse Transcriptase (Invitrogen) per manufacturer instructions. Quantitative PCR was carried out using SyBr Green PCR mastermix (Roche) and gene- or transposon-specific primers (see Table S4) on a Stratagene Mx real-time thermocycler.

DNA methylation analyses.

Whole genome BS-seq libraries were performed as previously described (*9*), except directly with pre-methylated final adapters. BS-seq data was mapped with BS seeker as previously described (*31*). For traditional bisulfite sequencing, genomic DNA extracted from two-week-old seedlings was bisulfite converted using MethylEasy (Human Genetic Signature) and processed as previously described (*5*). Primer sequences used for bisulfite sequencing are described in Table S4. Southern blot was performed as previously described (*2*).

H3K9me2 ChIP-seq analyses.

Two grams of 3-week-old seedlings were crosslinked with formaldehyde and chromatin-IP experiments were performed as previously described (*32*). A mouse monoclonal antibody was used for H3K9me2 immunoprecipitation (Abcam ab1220). ChIP-seq library was generated per manufacturer instructions (Illumina). Demultiplexed (by exact match to canonical 6-mers) single end 50-mer HiSeq PF-passing reads were aligned to the TAIR8 reference genome using Bowtie 1, keeping all hits with at most two or fewer mismatches in the first 28 cycles and with total sum of Phred quality scores at mismatches up to 100, further filtered to only keep reads with a unique hit of fewest total mismatches, retaining only that unique hit. Reads were extended downstream to total length 220 nucleotides to reflect nominal library fragment lengths and single-stranded per-base pair coverage tallied, normalized by total nuclear chromosome coverage to account for variation in sequencing depth.

siRNA analyses.

Total RNAs were extracted from flowers using Trizol (Ambion RNA technology) and siRNAs were purified as previously described (*33*) with the following modifications. Polyacrylamide gel-excised siRNAs were eluted in 0.3M NaCl overnight at 4°C. Gel debris were filtered using 5µm Filter tubes (IST Engineering Inc) and, ethanol-precipitated siRNAs were resuspended in 5ul of nuclease-free H_20 to subsequently generate libraries for High Throughput small RNA sequencing (TruSeq small RNA, Illumina) per manufacturer instruction. Small RNA libraries were Illumina sequenced to 50bp length, and resulting reads were trimmed for adapter sequences and then aligned to the TAIR8 genome using Bowtie (*28*).

Hi-C analyses.

Two grams of 3-week-old seedling leaves were crosslinked with formaldehyde as previously described (*32*). Hi-C experiments were performed as previously described (*34*), with the exception that plant nuclei were prepared following a previously published *Arabidopsis* ChIP protocol (*32*). Hi-C libraries were sequenced on a HiSeq 2000 sequencer (Illumina) obtaining paired end 50+50 nucleotide reads. Sequencing reads were mapped to the TAIR8 *A. thaliana* reference genome using Bowtie 1 to obtain all zero-mismatch hits of ends independently and keeping only paired end read pairs with each end having exactly one hit, obtaining 21,379,391 wild type and 14,815,038 *atmorc6-1* pairs. Paired reads with ends aligning to the same HindIII fragment were discarded. Hi-C interaction counts were summed within disjoint symmetric 2-D bins 200 kilobase pairs tiling the genome. HindIII fragments which overlapped regions of poor reference genome quality were excluded from the analysis. Genomic 1-D bins (rows and columns) in which > 50% of the sequence length was excluded by these filters were treated as missing data, excluded from further analyses, and appear in figures as empty regions. The "raw" coverage of each genomic 2-D bin was taken as the number of paired end reads lying in that bin. Whole genomic 1-D bins with a total coverage more than 3 standard deviations greater than or less than the mean were excluded and then the matrix of interactions was corrected for 1-D bin coverage variation as previously described (*34*) using 50 iterations of that procedure. The comparison between the wild type and *atmorc6-1* mutant was expressed as the difference divided by the mean within each bin with smoothing plus or minus one bin.

Immunofluorescence.

Immunofluorescence experiments examining chromocenter condensation were performed as previously described (*35*) with the following modifications. Leaves from three-week-old plants were fixed in 4% paraformaldehyde in TRIS buffer (10mM TRIS pH 7.5, 10mM EDTA, 100mM NaCl) for 20 minutes and washed twice in TRIS buffer. Leaves were chopped in 400 microliters lysis buffer (15mM TRIS pH 7.5, 2mM EDTA, 0.5mM spermine, 80mM KCl, 20mM NaCl, 0.1% Triton X-100) and filtered through a 35 micron cell strainer. Five microliters of nuclei suspension was added to sorting buffer (100mM TRIS pH 7.5, 50mM KCl, 2mM MgCl2, .05% Tween-20, 20.5% sucrose) and air dried on microscope slides for two hours and then

post-fixed in 4% paraformaldehyde in PBS for 20 minutes. Slides were washed three times in PBS and incubated in blocking buffer (3% BSA, 10% horse serum in PBS) for 30 minutes at 37°C. Nuclei were incubated at 4°C overnight in mouse monoclonal antibody against H3K9me2 (Abcam ab1220; 1:200). Slides were washed in PBS and incubated with goat anti-mouse FITC antibody (Abcam ab7064; 1:200) for 90 minutes at room temperature. Following PBS washes, nuclei were counterstained and mounted in Vectashield mounting media with DAPI (Vector H-1200). Nuclei were analyzed with a Zeiss Axio Imager Z1 microscope at 100X magnification and images were captured with a Hamamatsu ORCA-ER Camera. For detection of Myc epitope tagged proteins, nuclei were isolated as above. Following preparation of nuclei suspension, nuclei were spun down for 2 minutes at 2,000rpm and resuspended in PBS. Blocking and antibody incubations were performed in suspension, followed by pellet washing with PBS. Myc epitope was detected with mouse monoclonal antibody (Abcam 9E10; 1:200) and goat anti-mouse FITC (abcam ab7064; 1:200). Two microliters of prepared nuclei were mounted in Vectashield media. Nuclei were analyzed with the Applied Precision DeltaVision DV Live Cell Imaging System using Olympus IX-71 Customized Inverted Microscope and Photometrics CoolSNAP HQ2 CCD Camera (Figure 3). Additional images of nuclei were taken using a Zeiss LSM 510 META confocal microscope with Axiocam camera (Figure S15).

RNA interference in *C. elegans*.

RNAi experiments were carried out as reported previously (*36*) using the *eri-1(mg366); [wIs54(scm::gfp)]* strain, which shows increased sensitivity to RNAi. Briefly, bacterial strains carrying plasmids expressing double-stranded RNA targeting *morc-1* or *rde-4* were obtained from the Ahringer RNAi library (*37*). Hatched L1 *eri-1(mg366); [wIs54(scm::gfp)]* larvae were cultured on empty vector (L4440), *morc-1*, or *rde-4* RNAi bacteria for two generations at 22.5°C. Images of F_1 L4 larvae were captured on an Olympus BX61 epifluorescence compound microscope with a Hamamatsu ORCA ER camera using Slidebook 4.0.1 digital microscopy software (Intelligent Imaging Innovations) and processed using ImageJ.

Supplementary Figures:

Fig. S1. (**A**) Schematic representation of the *SDC::GFP* construct. The *SDC* promoter carries seven tandem repeats (black arrows) targeted by DNA methylation. The red bar corresponds to the *Simian Virus 40* (*SV40*) Nuclear Localization Signal fused to GFP. (**B**) Schematic of AtMORC1 and AtMORC6 proteins showing the GHKL and S5 ATPase domains together with putative Coiled-Coil (CC) domains. The location of nonsense mutations within the protein sequences is shown for each EMS allele. aa; amino acid. Based on contextual associations of prokaryotic and eukaryotic MORC family members with associated domains, as well as with genes in operons, eukaryotic MORCs were predicted to have originated from bacterial restriction modification systems, and in eukaryotes have been proposed to remodel chromatin superstructure in response to epigenetic signals such as histone and DNA methylation (*12*). For instance, topoisomerases and MutL (a factor involved in methylated DNA directed mismatch repair) proteins use ATP hydrolysis to mediate large movements and looping of DNA. Similar to other GHKL ATPases (*38*), MORC3 in mouse was shown to act as a molecular clamp, interacting with itself constitutively through its coiled-coil domain, and also interacting via its ATPase domain in an ATP-dependent manner (*39*). In this way, MORC protein architectures are also reminiscent of the structural maintenance of chromosomes (SMC) family of proteins, which control chromosome condensation and cohesion (*40*). In addition, a very distant class of ATPase homologs contain the GHKL domain fused with the hinge and coiled coil domains of SMC-like ATPases (*12*) one of which, SmcHD1, is required for maintenance of X chromosome inactivation in mouse (*41*). Interestingly, in *Arabidopsis*, the protein DMS3/IDN1, which contains an SMC-like Hinge domain,

has also been involved in gene silencing (*42, 43*) and GMI1, which is a GHKL protein carrying a Hinge domain has recently been involved in DNA repair (*44*).

Fig. S2. Mapping of *cmt3* #7, wt #67 and *cmt3* #49 mutations by bulk segregant analysis coupled with whole genome re-sequencing (*27*). (**A to C**) Depletion in percentage of Landsberg (L*er*) single nucleotide polymorphisms (SNPs), defining the linkage interval for the population *cmt3* #7 (chromosome 4 at ~17-18 megabases) (A), and defining the linkage intervals for the populations wt #67 (B) and *cmt3* #49 (C) (chromosome 1 at ~6-7 megabases). Red arrows mark the linkage intervals.

Fig. S3. Characterization of *atmorc1* and *atmorc6* EMS and T-DNA mutant alleles. (**A**) Location of EMS point mutations in *atmorc1-3*, *atmorc6-1*, and *atmorc6-2* alleles confirmed by traditional DNA sequencing. *AtMORC1* and *AtMORC6* reference sequences are shown for comparison. bp, base pair. (**B**) Gene structures of *AtMORC1* and *AtMORC6* showing exons (E, dark gray boxes) and introns (gray lanes). Light gray boxes correspond to 5' and 3' untranslated regions. The locations of EMS point mutations and T-DNA insertions are described above the gene structures. (**C** and **D**) Relative *AtMORC1* and *AtMORC6* RNA levels (C), and *SDC* RNA level (D) in *atmorc1-4* and *atmorc6-3* over wild type assayed by RT-qPCR and normalized to *ACTIN7*. Errors bars indicate standard deviation based on three independent biological replicates. Red arrows shown in (B) correspond to the primer locations within *AtMORC1* and *AtMORC6* mRNAs used in (C). (**E**) Genetic complementation tests and backcrosses showing that wt #67, *cmt3* #49, and *atmorc6-3* are three recessive allelic mutations in *AtMORC6* (top panels), while *cmt3* #7 and *atmorc1-4*

are two recessive allelic mutations in *AtMORC1* (two bottom left panels). The cross between wt #67 and *cmt3* #7 confirms that these two mutations are non-allelic (bottom right panel). Pictures represent leaves from F_1 plants observed under UV light for GFP fluorescence.

Fig. S4. Similar sets of TEs and protein-coding genes are upregulated in *atmorc1* and *atmorc6*. (**A**) Relative fold increase of *SDC* and four TE transcripts in *atmorc6-1*, *cmt3-11* and *cmt3-11 atmorc1-3* over wild type assayed by RT-qPCR and normalized to *ACTIN7*. Errors bars indicate standard deviation based on three independent biological replicates. (**B-D**) Venn diagrams showing overlap of upregulated TEs (B), upregulated protein-coding genes (C), and upregulated protein-coding genes associated with DNA methylation (D) in *atmorc1* and *atmorc6*. These analyses include the genes that were 4-fold up-regulated in RNA-seq experiments in both the EMS and T-DNA alleles. (**E**) Gene ontology (GO) analyses of genes upregulated in *atmorc1* and *atmorc6* showing no significant over-representation of any GO category in both *MORC* mutants. GO *p*-values are shown in parenthesis.

Fig. S5. DNA methylation at all protein-coding genes and transposons is not altered in *atmorc1* and *atmorc6.* (**A** and **B**) Metaplot analyses showing DNA methylation percent within protein-coding genes (A) and transposons (B) in *atmorc1-4*, *atmorc6-3* and wild type plants. The gray vertical lines mark the boundaries between 1 kilobase (Kb) upstream regions and gene bodies or transposons (left), and between gene bodies or transposons and 1Kb downstream regions (right).

Fig. S6. H3K9me2 is not altered in *atmorc1* and *atmorc6*. (**A**) $\log_2$ ratios of H3K9me2/H3 in *atmorc1-4* and *atmorc6-3* over wild type do not show H3K9me2 changes in *atmorc6* or *atmorc1* mutants at the *SDC* promoter region. The H3K9me2/H3 wild type ratio is shown over the *SDC* promoter region in which H3K9me2 is enriched. RNA-seq reads in the different genetic backgrounds are shown to define the *SDC* transcribed region. (**B**) Metaplot analyses showing $\log_2$ ratios of H3K9me2/H3 in *atmorc1-4* and *atmorc6-3* over wild type at the set of transposable elements and DNA-methylated genes that are upregulated in *atmorc1-4* and *atmorc6-3*. The gray vertical lines mark the boundaries between 1 kilobase upstream regions and transposons/PCGs (left) and between transposons/PCGs and 1 kilobase downstream regions (right). PCGs, Protein-coding genes.

Fig. S7. Small RNA accumulation is unaltered in *atmorc1* and *atmorc6*. Metaplot analyses showing no difference in the level of siRNAs in *atmorc1-4* and *atmorc6-3* compared to wild type at the set of transposable elements that are upregulated in *atmorc1-4* and *atmorc6-3*. The gray vertical lines mark the boundaries between 2 kilobases upstream regions and transposons (left) and between transposons and 2 kilobases downstream regions (right). Data is illustrated for different size classes of small RNAs.

Fig. S8. AtMORC1 and AtMORC6 are required for chromocenter condensation. Percentage of nuclei showing decondensed, partially decondensed (intermediate) and wild type chromocenters in *atmorc6-1*, *cmt3-11 atmorc1-3* and in *atmorc1-3 atmorc6-1* double mutants in comparison to control backgrounds after immunostaining of

nuclei using an antibody against H3K9me2. Pictures on top panels show examples of the three different patterns of chromocenters.

Fig. S9. H3K9me2 and DAPI staining show similar chromocenter condensation patterns in nuclei defined in Fig. S8 as nuclei showing wild type, intermediate or decondensed chromocenters in *cmt3-11 atmorc1-3*.

Fig. S10. H3K9me2 and DAPI staining show similar chromocenter condensation patterns in nuclei defined in Fig. S8 as nuclei showing wild type, intermediate or decondensed chromocenters in *atmorc6-1*.

Fig. S11. H3K9me2 and DAPI staining show similar chromocenter condensation patterns in nuclei defined in Fig. S8 as nuclei showing wild type, intermediate or decondensed chromocenters in *atmorc1-3 atmorc6-1*.

Fig. S12. Loci upregulated in *atmorc1* and *atmorc6* mostly localize to pericentromeric regions. Chromosomal views showing the $\log_2$ ratios (*atmorc6-3*/wild type and *atmorc1-4*/wild type) of RNA sequencing reads in 100 Kb bins. The two red bars on each chromosome delimit the pericentromeric region with white circles representing the centromeres.

Fig. S13. Interaction matrix of the *atmorc6-1* genome from Hi-C analysis. Positions along the 5 chromosomes are shown from left to right and top to bottom, and each pixel represents interactions from uniquely mapping paired end reads in 200 kilobase bins. Black bars and circles mark the positions of the pericentromeric and telomeric

regions, respectively. Light grey regions represent areas masked out due to problematic mapping. Black bars show separation between chromosomes.

Fig. S14. Myc tagged AtMORC1 and AtMORC6 complement the EMS mutant lines. (**A**) Western blot using an antibody against Myc confirms that pAtMORC1::AtMORC1-Myc and pAtMORC6::AtMORC6-Myc are expressed in transformed plants but not in untransformed control. (**B**) Similar analyses using an antibody against GFP show that lines expressing AtMORC1-Myc and AtMORC6-Myc do not express the *SDC::GFP* transgene, confirming that pAtMORC1::AtMORC1-Myc and pAtMORC6::AtMORC6-Myc proteins are functional. *cmt3-11 atmorc1-3* and *atmorc6-1* mutants are used as GFP positive controls for AtMORC1-Myc and AtMORC6-Myc complementation, respectively. Coomassie staining of the large Rubisco subunit (rbcL) is used as loading control.

Fig. S15. AtMORC6 bodies are adjacent to chromocenters. Additional images of nuclei expressing AtMORC6-Myc were obtained using a Zeiss LSM 510 META confocal microscope. Eight images are displayed, taken at depth intervals of 1 micron. Multiple chromocenters are bordered by AtMORC6 bodies.

Fig. S1

A


SDCpro
GFP

B

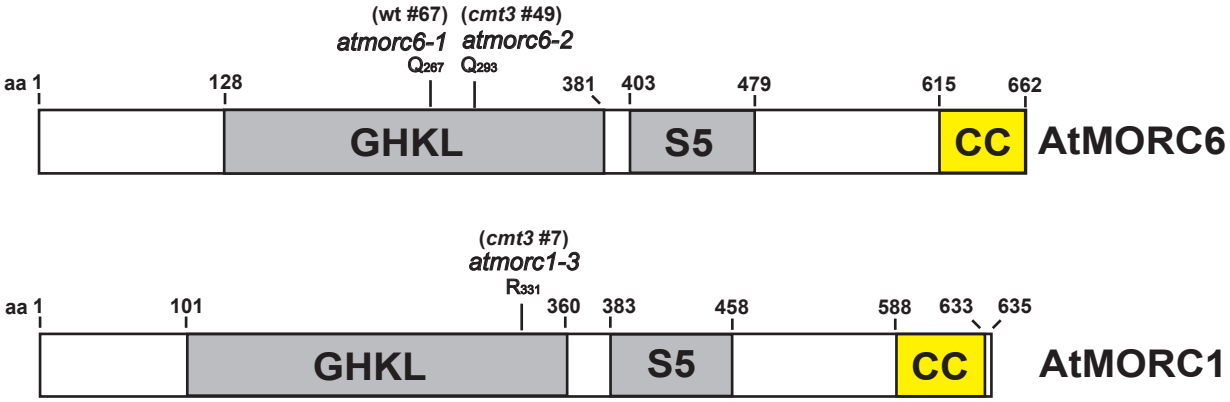
(wt #67)
atmorc6-1
Q267
(cmt3 #49)
atmorc6-2
Q293
aa 1
128
381
403
479
615
662
GHKL
S5
CC
AtMORC6
(cmt3 #7)
atmorc1-3
R331
aa 1
101
360
383
458
588
633
635
GHKL
S5
CC
AtMORC1

Fig. S2

A

cmt3 #7 (atmorc1-3)

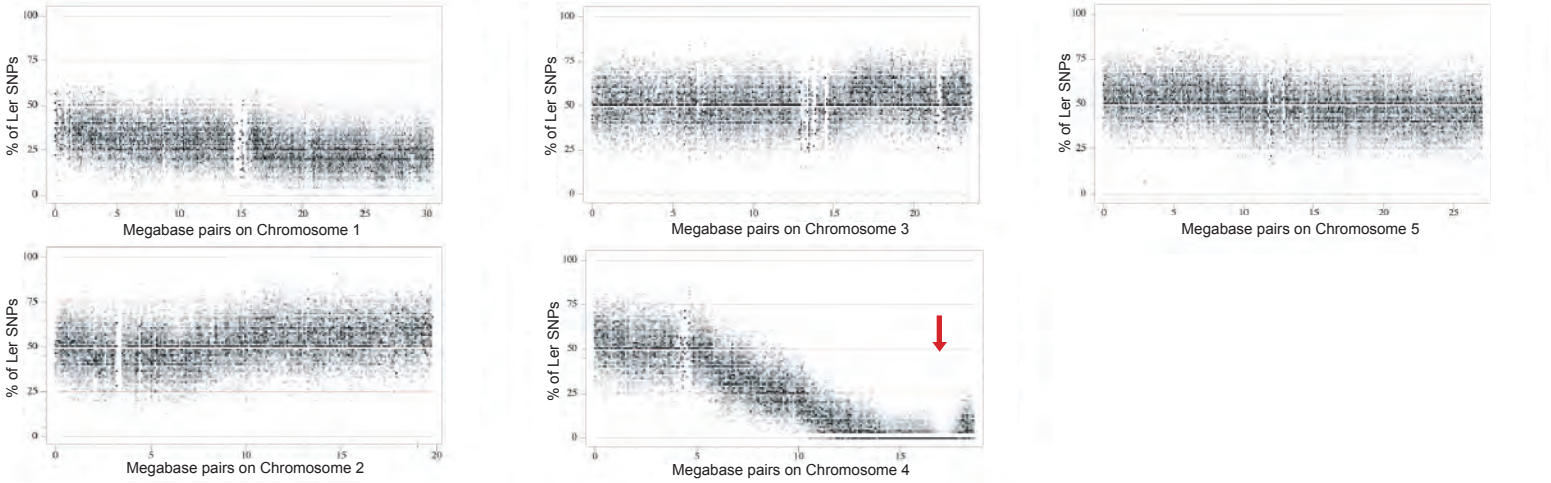

B

wt *#67 (atmorc6-1)*

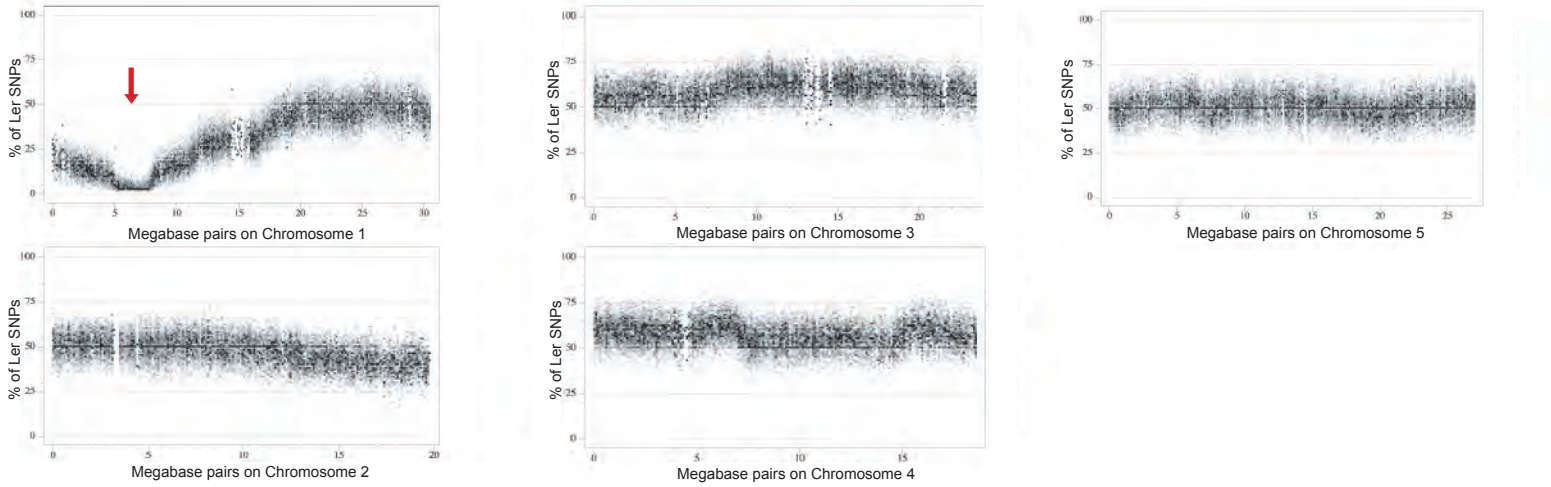

C

cmt3 #49 (atmorc6-2)

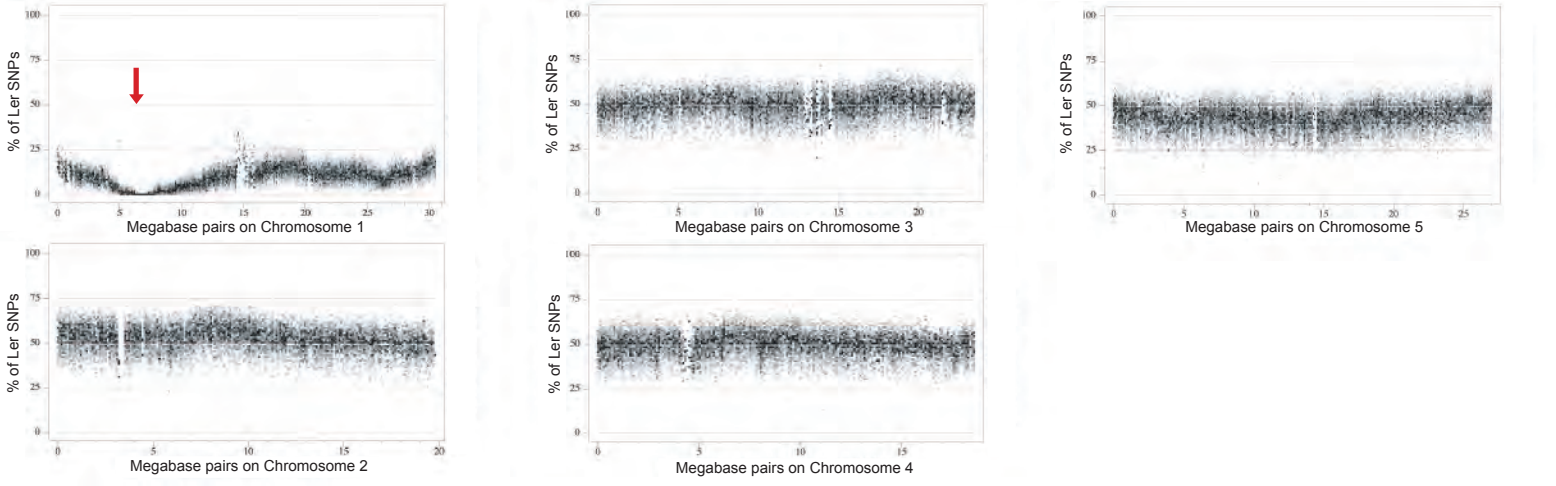

Fig. S3

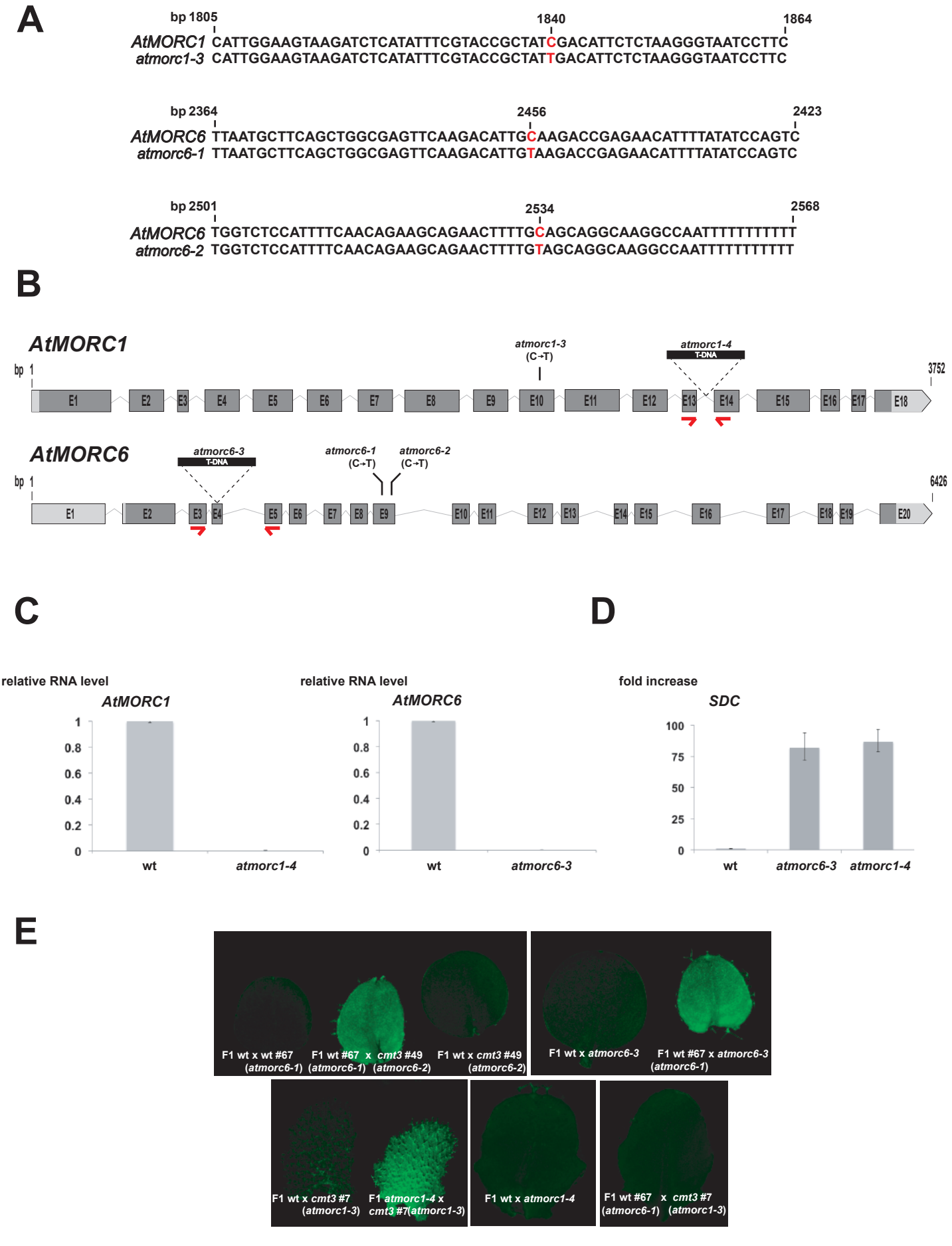
A
bp 1805
1840
1864
AtMORC1 CATTGGAAGTAAGATCTCATATTTCGTACCGCTATCGACATTCTCTAAGGGTAATCCTTC
atmorc1-3 CATTGGAAGTAAGATCTCATATTTCGTACCGCTATTGACATTCTCTAAGGGTAATCCTTC
bp 2364
2456
2423
AtMORC6 TTAATGCTTCAGCTGGCGAGTTCAAGACATTGCAAGACCGAGAACATTTTATATCCAGTC
atmorc6-1 TTAATGCTTCAGCTGGCGAGTTCAAGACATTGTAAGACCGAGAACATTTTATATCCAGTC
bp 2501
2534
2568
AtMORC6 TGGTCTCCATTTTCAACAGAAGCAGAACTTTTGCAGCAGGCAAGGCCAATTTTTTTTTTT
atmorc6-2 TGGTCTCCATTTTCAACAGAAGCAGAACTTTTGTAGCAGGCAAGGCCAATTTTTTTTTTT
B
AtMORC1
bp 1
atmorc1-3 (C→T)
atmorc1-4 T-DNA
3752
E1 E2 E3 E4 E5 E6 E7 E8 E9 E10 E11 E12 E13 E14 E15 E16 E17 E18
AtMORC6
atmorc6-3 T-DNA
atmorc6-1 (C→T)
atmorc6-2 (C→T)
bp 1
6426
E1 E2 E3 E4 E5 E6 E7 E8 E9 E10 E11 E12 E13 E14 E15 E16 E17 E18 E19 E20
C
relative RNA level
AtMORC1
1 0.8 0.6 0.4 0.2 0
wt
atmorc1-4
relative RNA level
AtMORC6
1 0.8 0.6 0.4 0.2 0
wt
atmorc6-3
D
fold increase
SDC
100 75 50 25 0
wt
atmorc6-3
atmorc1-4
E
F1 wt x wt #67 (atmorc6-1)
F1 wt #67 x cmt3 #49 (atmorc6-1)
F1 wt x cmt3 #49 (atmorc6-2)
F1 wt x atmorc6-3
F1 wt #67 x atmorc6-3 (atmorc6-1)
F1 wt x cmt3 #7 (atmorc1-3)
F1 atmorc1-4 x cmt3 #7(atmorc1-3)
F1 wt x atmorc1-4
F1 wt #67 x cmt3 #7 (atmorc6-1) (atmorc1-3)

Fig. S4

A

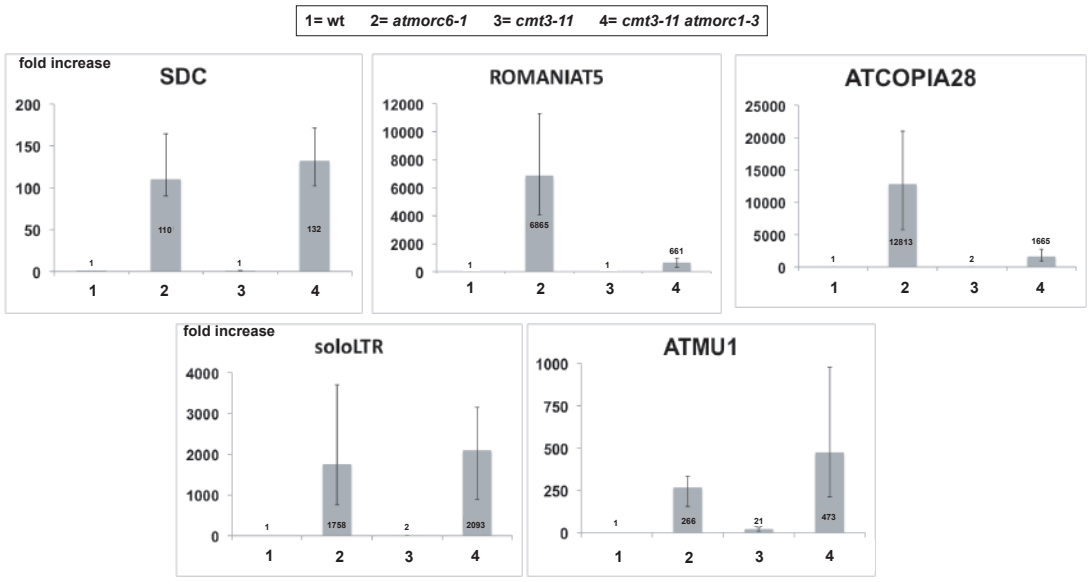
1= wt 2= atmorc6-1 3= cmt3-11 4= cmt3-11 atmorc1-3
fold increase
SDC
ROMANIAT5
ATCOPIA28
soloLTR
ATMU1

B

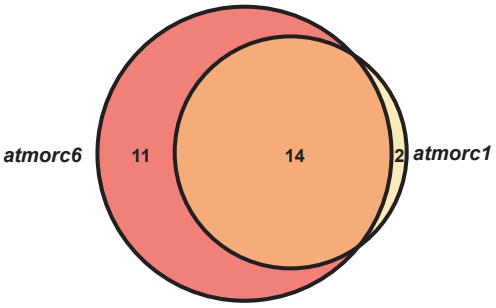
Transposable Elements
atmorc6
11
14
2
atmorc1

C

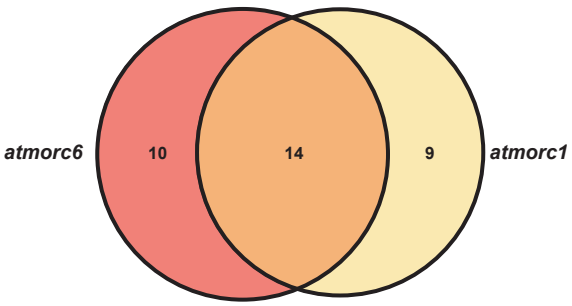
Protein coding Genes
atmorc6
10
14
9
atmorc1

D

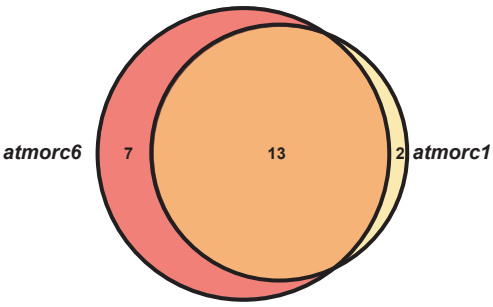
DNA-Methylated Protein coding Genes
atmorc6
7
13
2
atmorc1

E

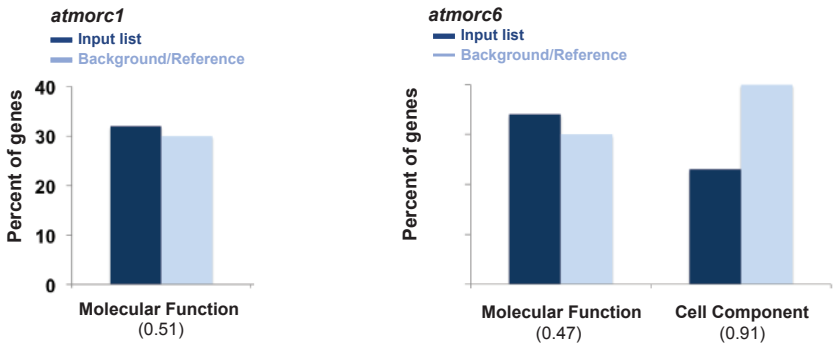
atmorc1
Input list
Background/Reference
Percent of genes
Molecular Function
(0.51)
atmorc6
Input list
Background/Reference
Percent of genes
Molecular Function
(0.47)
Cell Component
(0.91)

Fig. S5

A

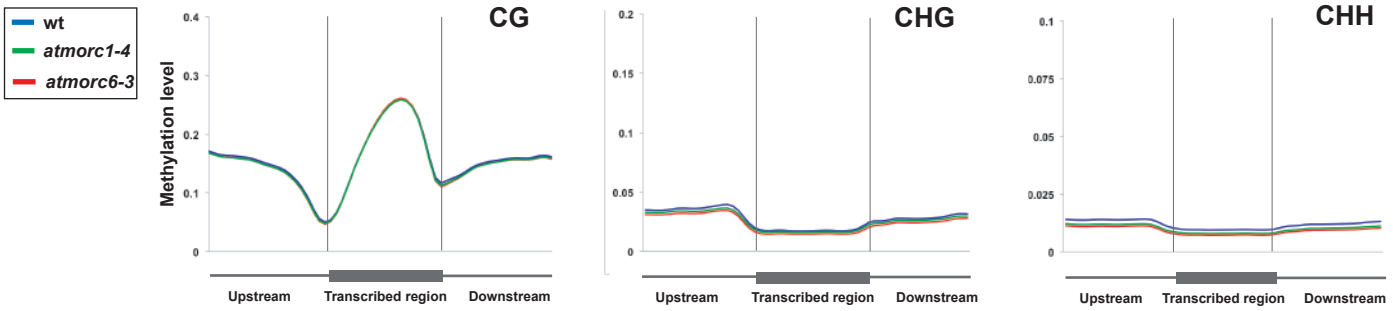
wt
atmorc1-4
atmorc6-3
Methylation level
CG
CHG
CHH
Upstream
Transcribed region
Downstream

B

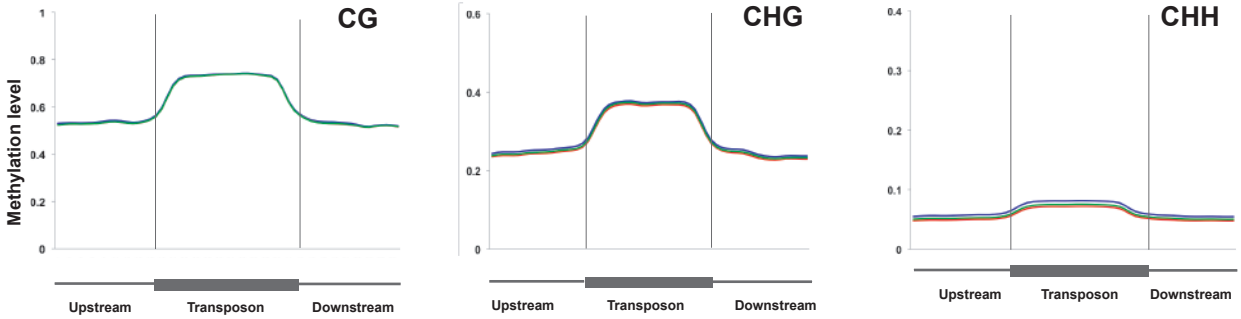
Methylation level
CG
CHG
CHH
Upstream
Transposon
Downstream

Fig. S6

A

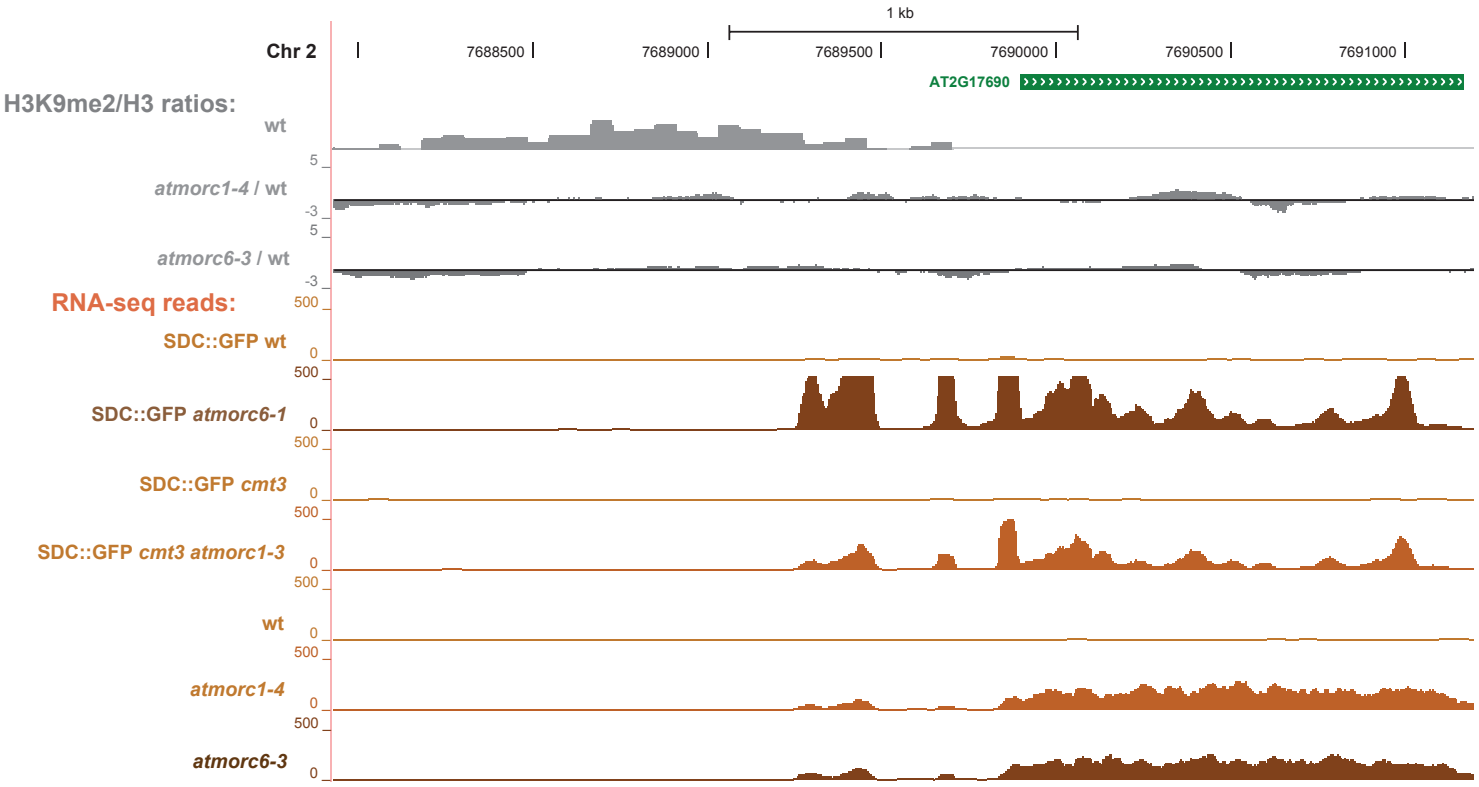
1 kb
Chr 2
7688500
7689000
7689500
7690000
7690500
7691000
AT2G17690
H3K9me2/H3 ratios:
wt
atmorc1-4 / wt
atmorc6-3 / wt
RNA-seq reads:
SDC::GFP wt
SDC::GFP atmorc6-1
SDC::GFP cmt3
SDC::GFP cmt3 atmorc1-3
wt
atmorc1-4
atmorc6-3

B

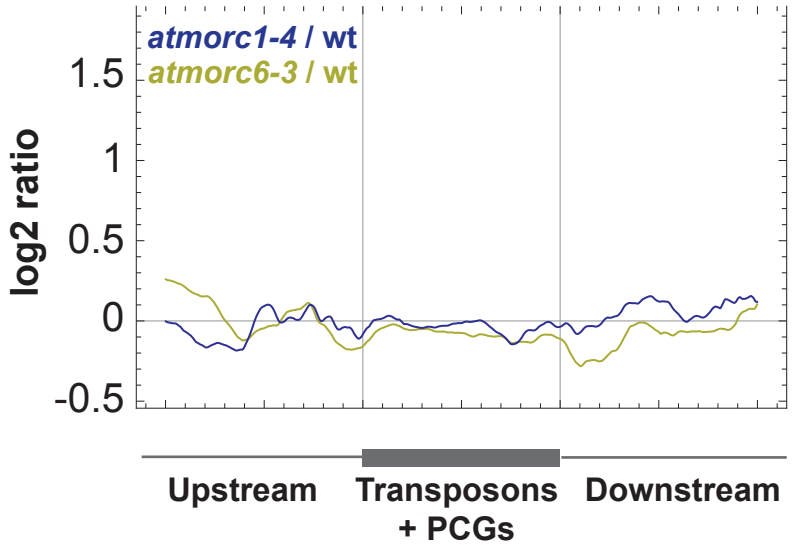
atmorc1-4 / wt
atmorc6-3 / wt
log2 ratio
1.5
1
0.5
0
-0.5
Upstream
Transposons
+ PCGs
Downstream

Fig. S7

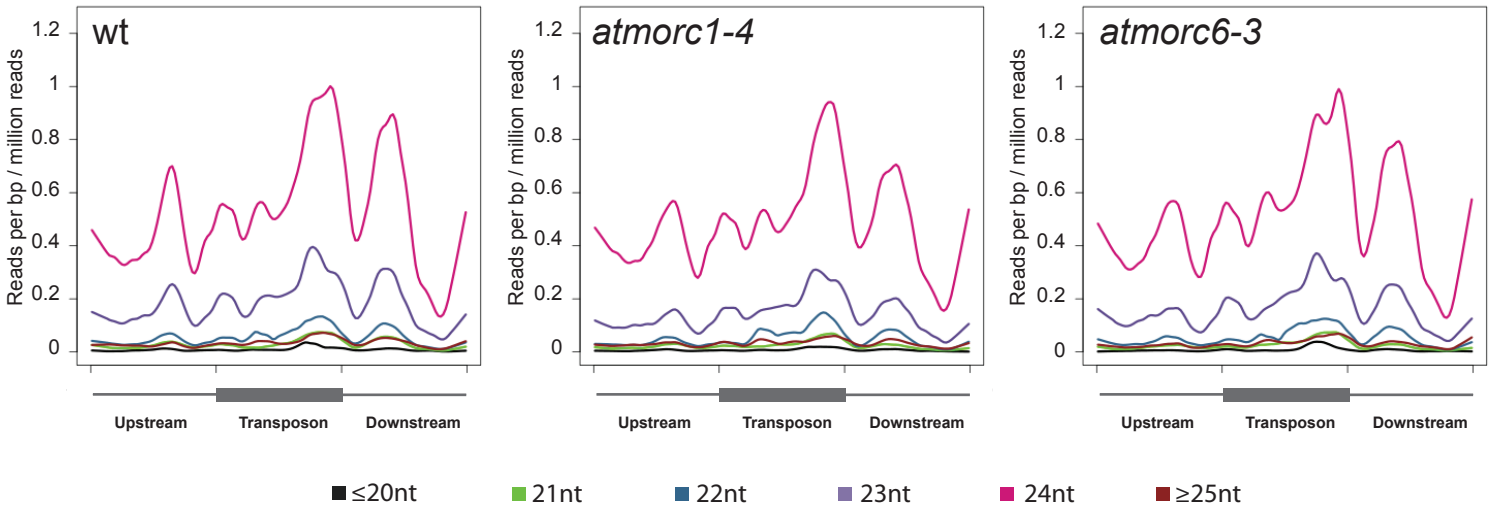
wt
atmorc1-4
atmorc6-3
Reads per bp / million reads
1.2
1
0.8
0.6
0.4
0.2
0
Upstream
Transposon
Downstream
≤20nt
21nt
22nt
23nt
24nt
≥25nt

Fig. S8

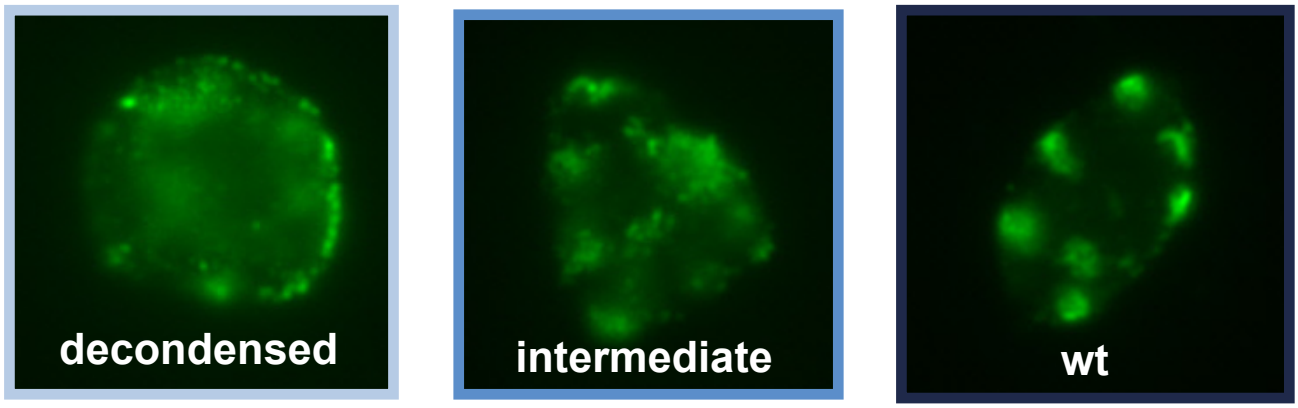
decondensed
intermediate
wt

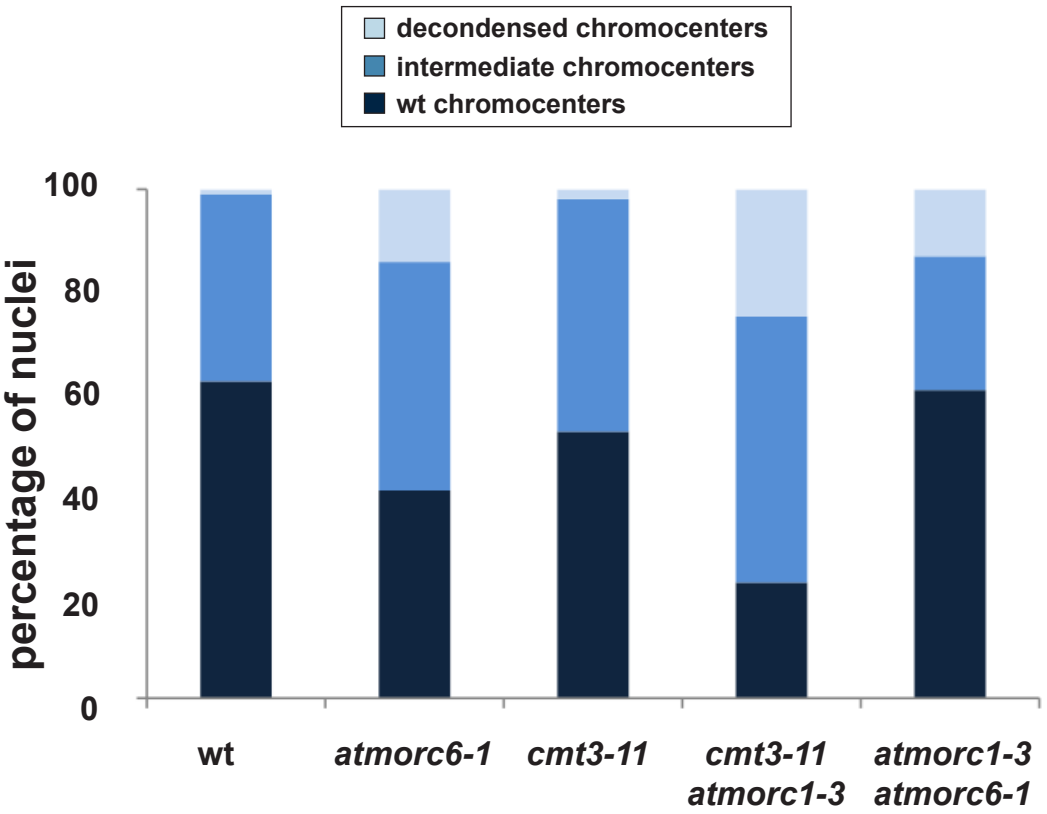
decondensed chromocenters
intermediate chromocenters
wt chromocenters
percentage of nuclei
100
80
60
40
20
0
wt
atmorc6-1
cmt3-11
cmt3-11 atmorc1-3
atmorc1-3 atmorc6-1

Fig. S9

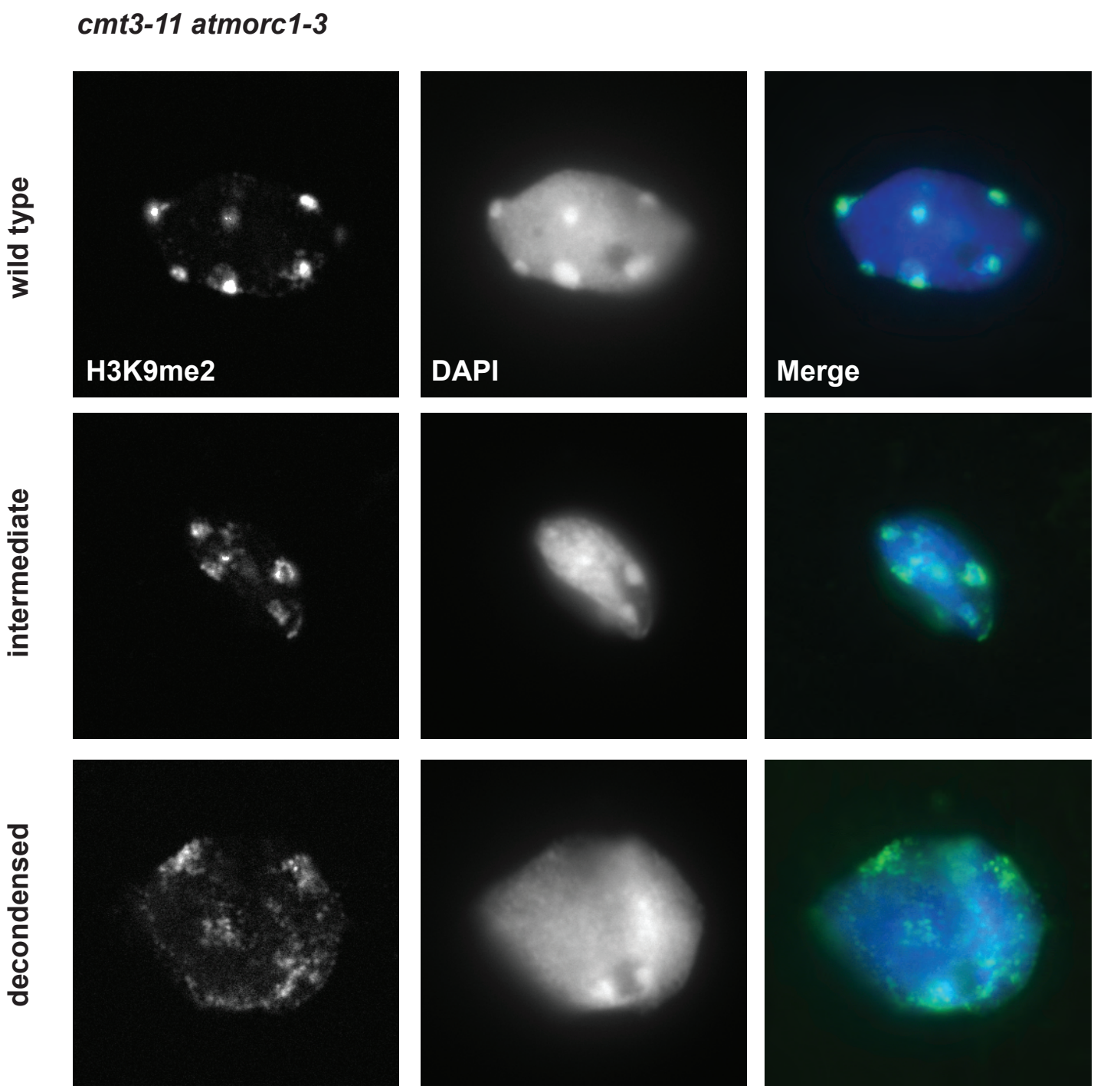
cmt3-11 atmorc1-3
wild type
intermediate
decondensed
H3K9me2
DAPI
Merge

Fig. S10

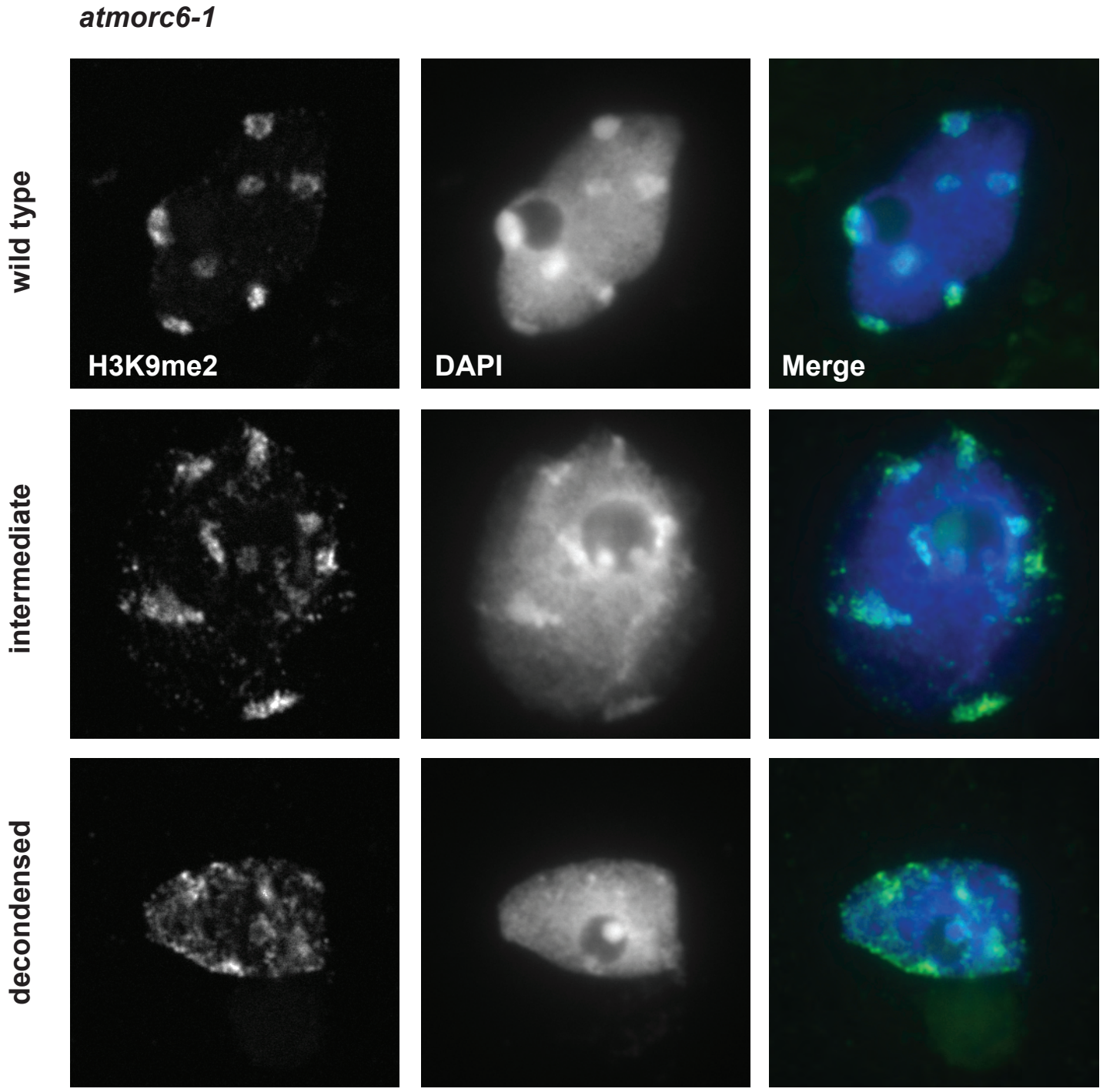
atmorc6-1
wild type
intermediate
decondensed
H3K9me2
DAPI
Merge

Fig. S11

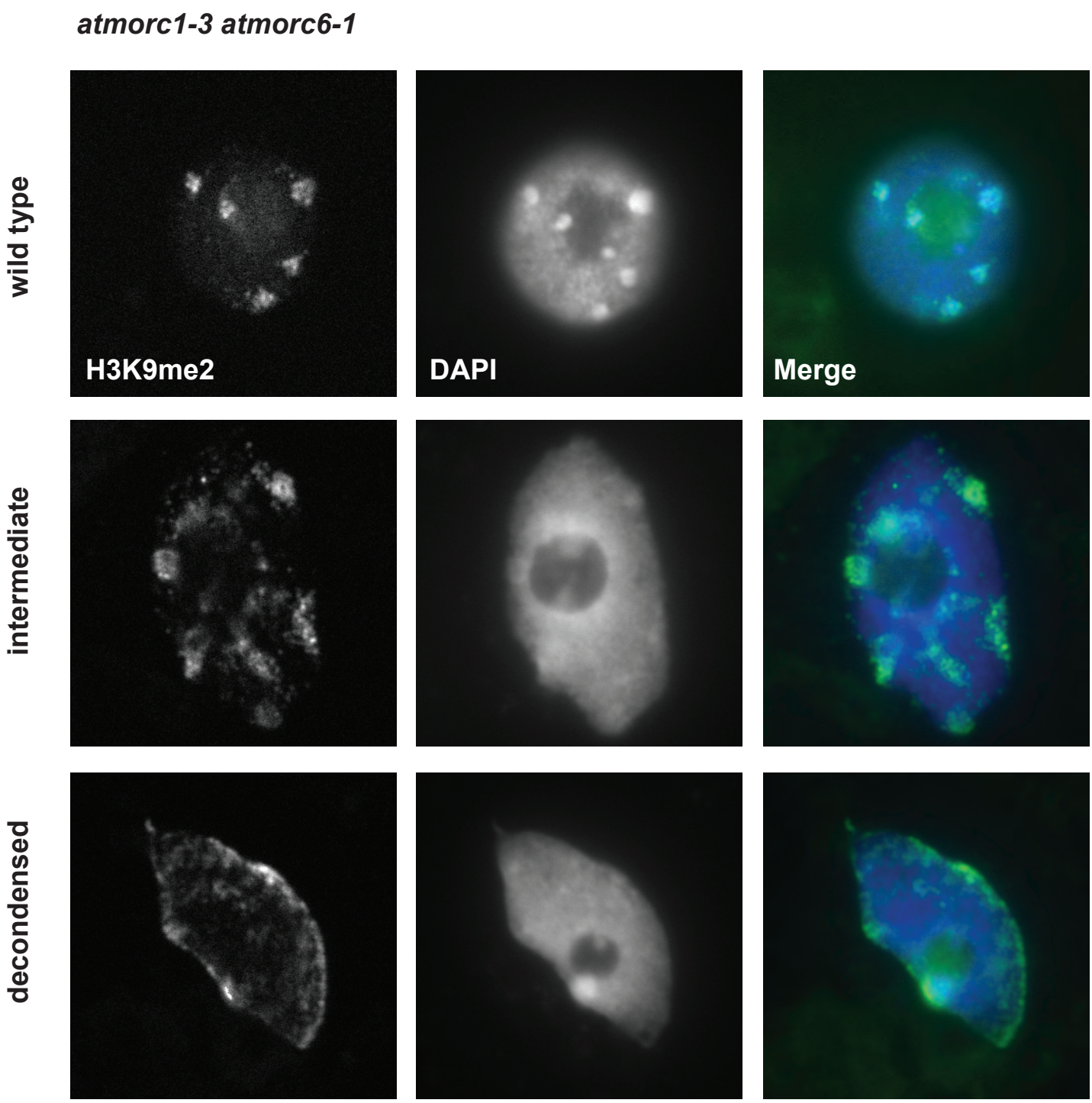
atmorc1-3 atmorc6-1
wild type
intermediate
decondensed
H3K9me2
DAPI
Merge

Fig. S12

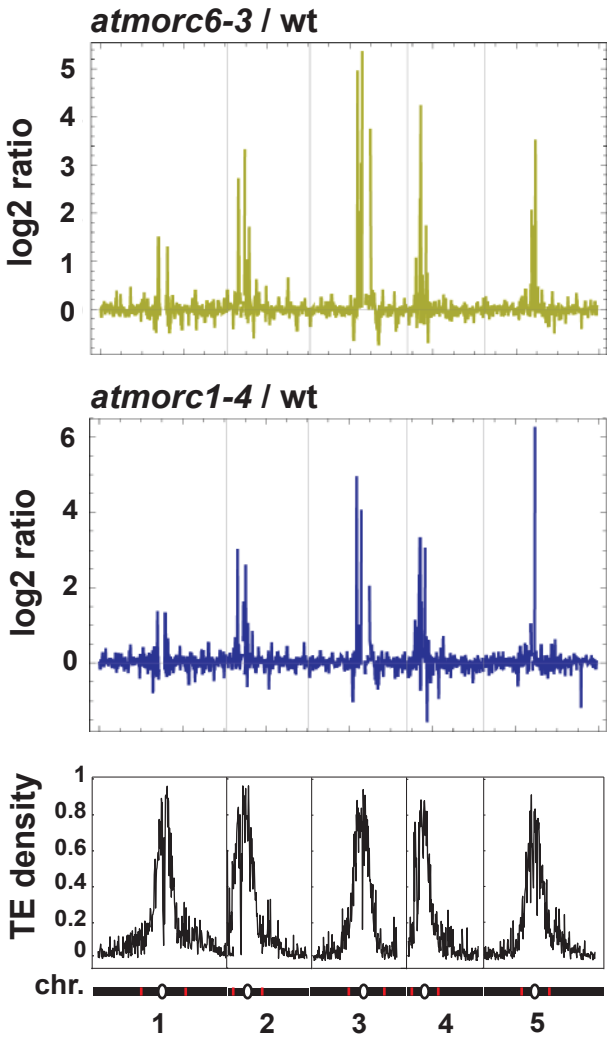
atmorc6-3 / wt
log2 ratio
5
4
3
2
1
0
atmorc1-4 / wt
log2 ratio
6
4
2
0
TE density
1
0.8
0.6
0.4
0.2
0
chr.
1
2
3
4
5

Fig. S13

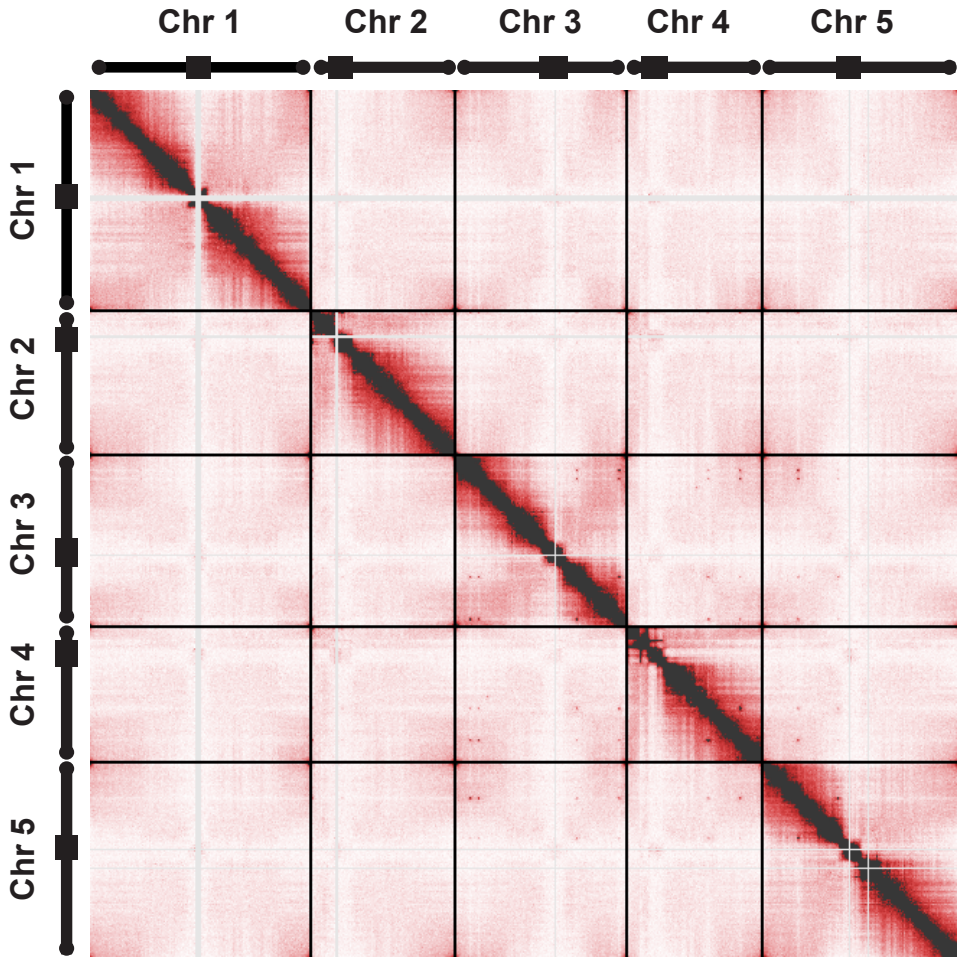

Fig. S14

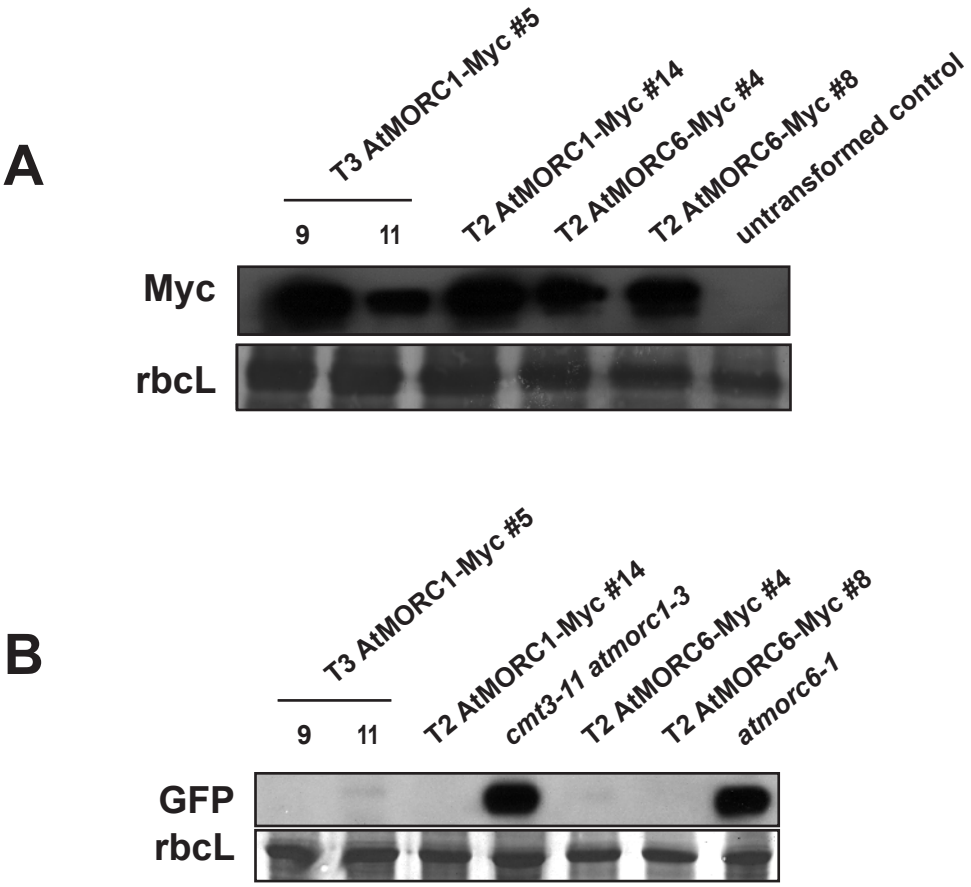
A
T3 AtMORC1-Myc #5
9
11
T2 AtMORC1-Myc #14
T2 AtMORC6-Myc #4
T2 AtMORC6-Myc #8
untransformed control
Myc
rbcL
B
T3 AtMORC1-Myc #5
9
11
T2 AtMORC1-Myc #14
cmt3-11 atmorc1-3
T2 AtMORC6-Myc #4
T2 AtMORC6-Myc #8
atmorc6-1
GFP
rbcL

Fig. S15

pAtMORC6::AtMORC6-Myc

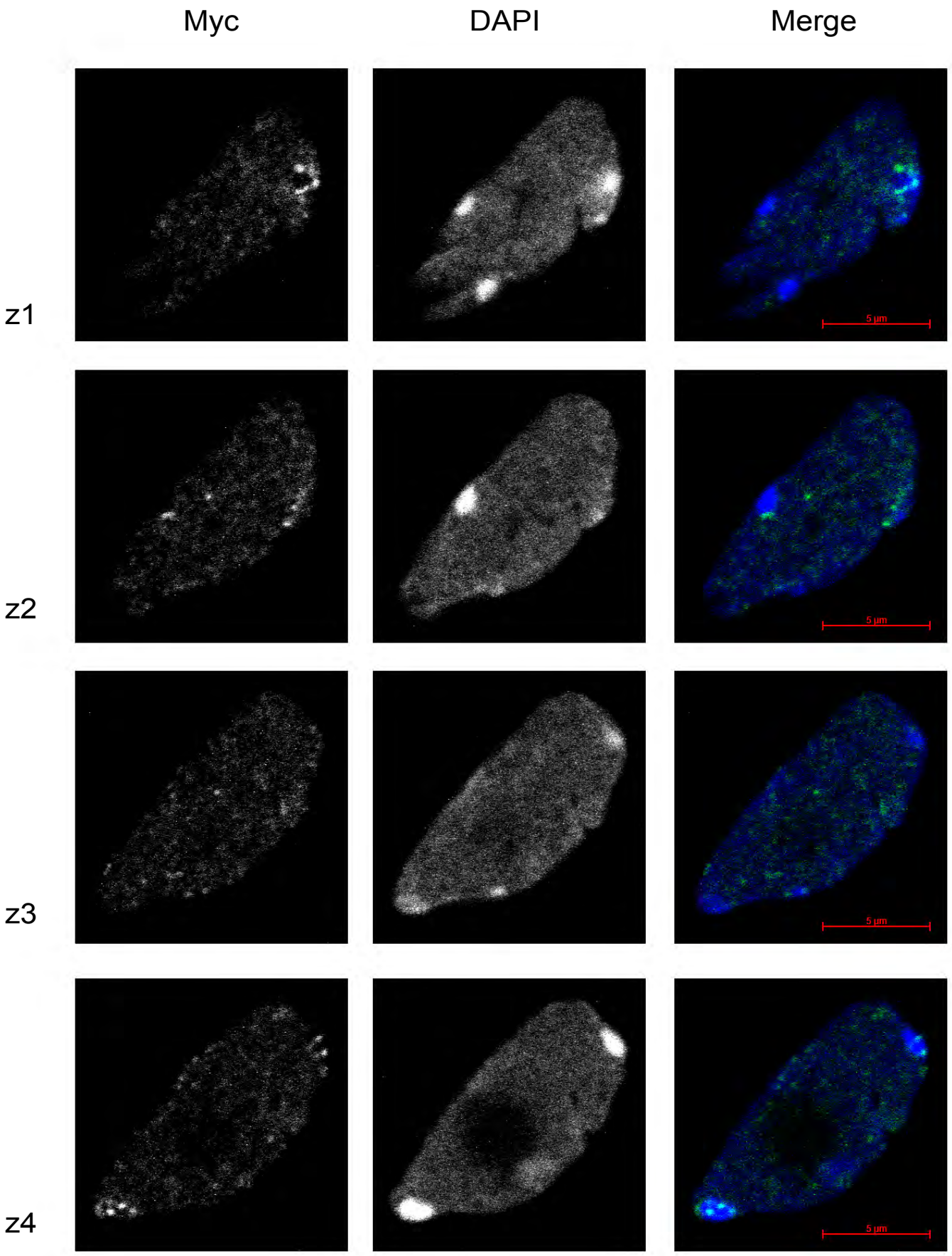

Fig. S15 (continued)

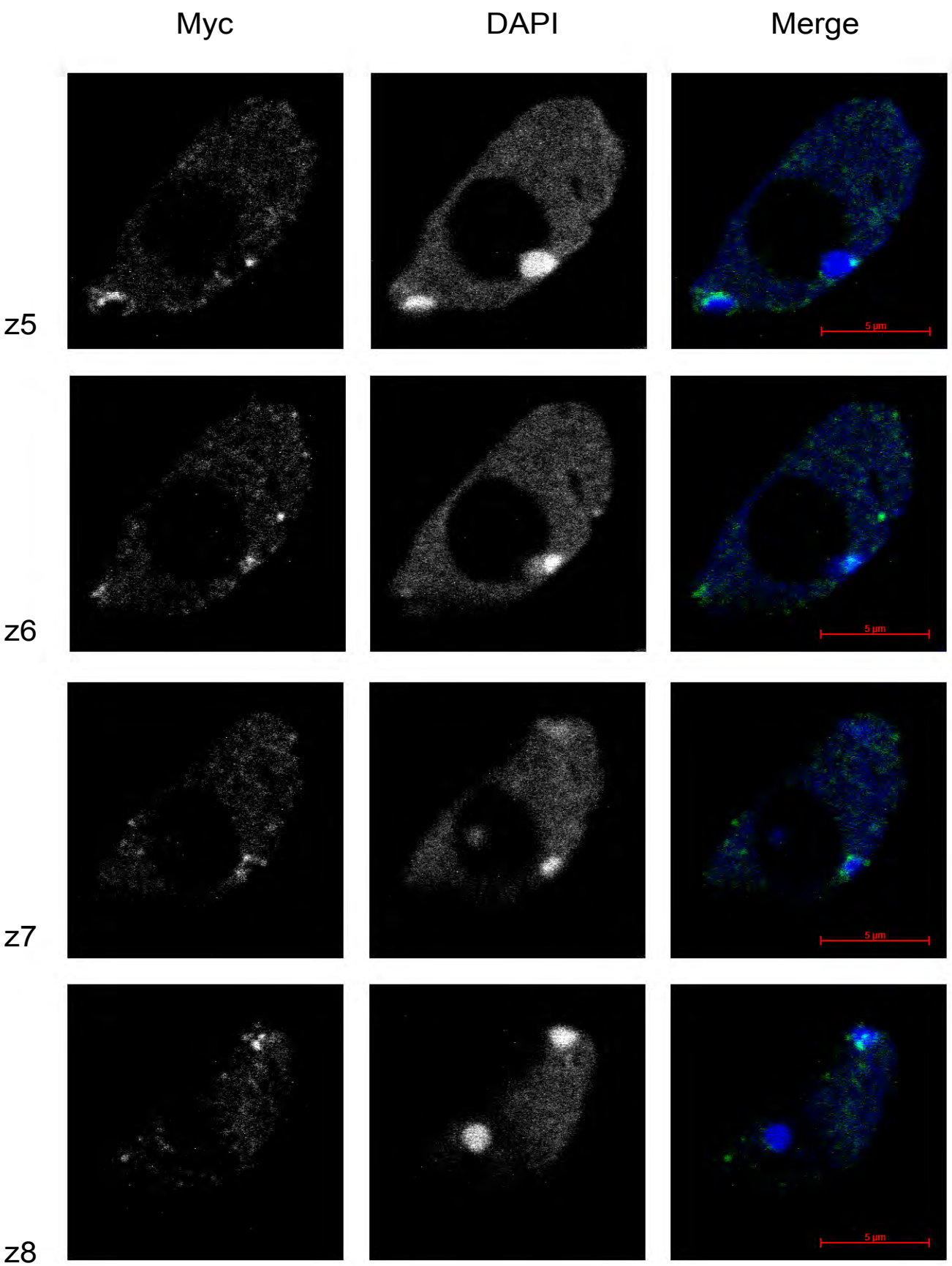

Table S1: Lists of Transposable elements (TEs) 4-fold upregulated in both EMS and T-DNA *atmorc6* and *atmorc1* mutant alleles. The TE soloLTR was identified by RT-qPCR. Therefore, it does not appear in Venn diagram shown in Fig. S4b.

TEs upregulated in *atmorc6*			
NAME	FAMILY NAME	SUPERFAMILY NAME	CHROMOSOMAL LOCATION
AT1TE43225	ROMANIAT5	LTR/Copia	chr1:13,232,205-13,236,935
AT1TE45510	ATENSPM6	DNA/En-Spm	chr1:13,872,370-13,872,595
AT1TE51360	ROMANIAT5	LTR/Copia	chr1:15,613,068-15,617,844
AT2TE07145	ATCOPIA95	LTR/Copia	chr2:1,547,658-1,552,030
AT2TE13060	ATCOPIA32	LTR/Copia	chr2:2,995,748-2,996,367
AT2TE16220	HELITRON2	RC/Helitron	chr2:3,749,179-3,756,447
AT2TE18240	ATIS112A	DNA/Harbinger	chr2:4,343,480-4,344,832
AT2TE28020	ATMU1	DNA/MuDR	chr2:6,888,343-6,891,692
AT2TE41170	ATIS112A	DNA/Harbinger	chr2:9,660,885-9,661,799
AT3TE51895	ROMANIAT5	LTR/Copia	chr3:12,605,745-12,609,307
AT3TE51900	ATCOPIA28	LTR/Copia	chr3:12,609,702-12,610,774
AT3TE51910	VANDAL18NA	DNA/MuDR	chr3:12,612,304-12,613,201
AT3TE51930	ATGP1	LTR/Gypsy	chr3:12,615,787-12,623,418
AT3TE60425	ATHILA3	LTR/Gypsy	chr3:14,799,085-14,800,505
AT3TE60460	ATHILA6A	LTR/Gypsy	chr3:14,806,306-14,815,940
AT3TE63540	ATHILA2	LTR/Gypsy	chr3:15,722,463-15,733,680
AT4TE04415	ATIS112A	DNA/Harbinger	chr4:860,921-864,078
AT4TE09845	ATIS112A	DNA/Harbinger	chr4:2,076,980-2,077,351
AT4TE15005	ATHILA3	LTR/Gypsy	chr4:3,266,370-3,288,501
AT4TE15025	ATHILA0_I	LTR/Gypsy	chr4:3,273,946-3,285,539
AT4TE15030	ATHILA6A	LTR/Gypsy	chr4:3,274,431-3,285,232
soloLTR	soloLTR	retroelement soloLTR	chr5:9,871,837-9,872,408
AT5TE39630	ATIS112A	DNA/Harbinger	chr5:10,901,855-10,903,021
AT5TE47200	ATHILA2	LTR/Gypsy	chr5:13,334,474-13,345,770
AT5TE48715	ATREP15	RC/Helitron	chr5:13,705,744-13,706,653
AT5TE48720	HELITRONY1E	RC/Helitron	chr5:13,706,654-13,706,934
TEs upregulated in *atmorc1*			
NAME	FAMILY NAME	SUPERFAMILY NAME	CHROMOSOMAL LOCATION
AT1TE43225	ROMANIAT5	LTR/Copia	chr1:13,232,205-13,236,935
AT1TE45510	ATENSPM6	DNA/En-Spm	chr1:13,872,370-13,872,595
AT1TE51360	ROMANIAT5	LTR/Copia	chr1:15,613,068-15,617,844
AT2TE13060	ATCOPIA32	LTR/Copia	chr2:2,995,748-2,996,367
AT2TE18240	ATIS112A	DNA/Harbinger	chr2:4,343,480-4,344,832
AT2TE28020	ATMU1	DNA/MuDR	chr2:6,888,343-6,891,692
AT2TE28025	ATGP10	LTR/Gypsy	chr2:6,891,693-6,892,236
AT3TE51895	ROMANIAT5	LTR/Copia	chr3:12,605,745-12,609,307
AT3TE51900	ATCOPIA28	LTR/Copia	chr3:12,609,702-12,610,774
AT3TE60460	ATHILA6A	LTR/Gypsy	chr3:14,806,306-14,815,940
AT4TE04415	ATIS112A	DNA/Harbinger	chr4:860,921-864,078
AT4TE09845	ATIS112A	DNA/Harbinger	chr4:2,076,980-2,077,351
soloLTR	soloLTR	retroelement soloLTR	chr5:9,871,837-9,872,408
AT5TE39630	ATIS112A	DNA/Harbinger	chr5:10,901,855-10,903,021
AT5TE48715	ATREP15	RC/Helitron	chr5:13,705,744-13,706,653
AT5TE48720	HELITRONY1E	RC/Helitron	chr5:13,706,654-13,706,934

AT5TE48740	ATLINE1_4	LINE/L1	chr5:13,712,007-13,715,840

Table S2: Lists of Protein coding genes 4-fold upregulated in both EMS and T-DNA *atmorc6* and *atmorc1* mutant alleles. With the exception of genes in italics, all genes in these lists are located in pericentromeric regions and show DNA methylation or H3K9me2 silencing marks.

Protein coding genes upregulated in *atmorc6*	
NAME	GENE ANNOTATION
AT1G33840	unknown protein
AT1G35730	APUM9 (ARABIDOPSIS PUMILIO 9); RNA binding
AT1G36675	glycine-rich protein
AT1G53480	unknown protein
AT1G59930	unknown protein
AT1G60110	jacalin lectin family protein
AT1G67105	non coding RNA
AT2G07215	unknown protein
AT2G07240	Ulp1 protease family protein
AT2G10975	unknown protein
AT2G13770	unknown protein
AT2G17690	SDC, F-box family protein
AT3G20340	*unknown protein*
AT3G29639	unknown protein
AT3G30842	ATPDR10/PDR10 (PLEIOTROPIC DRUG RESISTANCE 10)
AT3G33528	unknown protein
AT3G42850	galactokinase, putative
AT4G12490	*protease inhibitor/seed storage/lipid transfer protein (LTP) family protein*
AT5G07550	GRP19 (Glycine rich protein 19)
AT5G07560	GRP20 (Glycine rich protein 20); nutrient reservoir
AT5G15500	*ankyrin repeat family protein*
AT5G35480	unknown protein
AT5G35490	unknown protein
AT5G36910	*THI2.2 (THIONIN 2.2); toxin receptor binding (THI2.2)*
Protein coding genes upregulated in *atmorc1*	
NAME	GENE ANNOTATION
AT1G19610	*LCR78/PDF1.4 (Low-molecular-weight cysteine-rich 78)*
AT1G26390	*FAD-binding domain-containing protein*
AT1G26410	*FAD-binding domain-containing protein*
AT1G33840	unknown protein
AT1G35730	APUM9 (ARABIDOPSIS PUMILIO 9)
AT1G36675	glycine-rich protein (AT1G36675)
AT1G47890	*disease resistance family protein*
AT2G07215	unknown protein
AT2G10975	unknown protein
AT2G13770	unknown protein
AT2G17690	SDC, F-box family protein
AT2G17740	*DC1 domain-containing protein*
AT2G45220	*pectinesterase family protein*
AT3G29639	unknown protein
AT3G30842	ATPDR10/PDR10 (PLEIOTROPIC DRUG RESISTANCE 10)
AT3G33528	unknown protein
AT3G55970	oxidoreductase, 2OG-Fe(II) oxygenase family protein

AT4G12490	*protease inhibitor/seed storage/lipid transfer protein (LTP) family protein*
AT4G18170	*WRKY28 (WRKY DNA-binding protein 28); transcription factor*
AT5G07550	GRP19 (Glycine rich protein 19)
AT5G35480	unknown protein
AT5G35490	unknown protein
AT5G35510	unknown protein

Table S3: Lists of Transposable elements (TEs) and protein-coding genes (PCGs) that were 4-fold upregulated in the *atmorc1-3 atmorc6-1* double mutant. * defines loci found to be 4-fold upregulated only in the *atmorc1-3 atmorc6-1* double and not in the *atmorc1* or *atmorc6* single mutants. All the other loci have been found to be upregulated in either EMS or T-DNA *atmorc1* and/or *atmorc6* alleles at least in one RNA sequencing dataset.

TEs upregulated in the *atmorc1-3 atmorc6-1* double mutant			
NAME	FAMILY NAME	SUPERFAMILY NAME	CHROMOSOMAL LOCATION
AT1TE30845	HELITRON1	RC/Helitron	chr1:9,574,349-9,575,358
AT1TE43225	ROMANIAT5	LTR/Copia	chr1:13,232,205-13,236,935
AT1TE45135	ATHILA2	LTR/Gypsy	chr1:13,872,370-13,872,595
AT1TE45510	ATENSPM6	DNA/En-Spm	chr1:13,872,370-13,872,595
AT1TE53070	ATCOPIA87	LTR/Copia	chr1:16,118,258-16,118,383
AT1TE59745	ATCOPIA49	LTR/Copia	chr1:18,005,845-18,011,038
AT2TE07145	ATCOPIA95	LTR/Copia	chr2:1,547,658-1,552,030
AT2TE08840	TA11	LINE/L1	chr2:1,921,517-1,925,279
AT2TE13060	ATCOPIA32	LTR/Copia	chr2:2,995,748-2,996,367
AT2TE15415	ATGP10	LTR/Gypsy	chr2:3,533,343-3,539,331
AT2TE15880	ATHILA6A	LTR/Gypsy	chr2:3,643,453-3,652,409
AT2TE16220	HELITRON2	RC/Helitron	chr2:3,749,179-3,756,447
AT2TE18240	ATIS112A	DNA/Harbinger	chr2:4,343,480-4,344,832
AT2TE19615	VANDAL21	DNA/MuDR	chr2:4,736,486-4,744,627
AT2TE19625	ATHILA4C	LTR/Gypsy	chr2:4,738,315-4,739,542
AT2TE29450	ATCOPIA70	LTR/Copia	chr2:7,231,166-7,236,206
AT2TE38900	ATCOPIA76	LTR/Copia	chr2:9,194,572-9,198,735
AT2TE38905	ATGP2N	LTR/Gypsy	chr2:9,198,736-9,200,805
AT2TE66360	ATCOPIA50	LTR/Copia	chr2:14,938,850-14,939,092
AT3TE50570	VANDAL3	DNA/MuDR	chr3:12,177,936-12,189,847
AT3TE50595	ATHILA2	LTR/Gypsy	chr3:12,189,865-12,193,865
AT3TE51895	ROMANIAT5	LTR/Copia	chr3:12,605,745-12,609,307
AT3TE51900	ATCOPIA28	LTR/Copia	chr3:12,609,702-12,610,774
AT3TE51910	VANDAL18NA	DNA/MuDR	chr3:12,612,304-12,613,201
AT3TE51930	ATGP1	LTR/Gypsy	chr3:12,615,787-12,623,418
AT3TE60425	ATHILA3	LTR/Gypsy	chr3:14,799,08- 14,800,505
AT3TE60460	ATHILA6A	LTR/Gypsy	chr3:14,806,306-14,815,940
AT3TE63540	ATHILA2	LTR/Gypsy	chr3:15,722,463-15,733,680
AT4TE09845	ATIS112A	DNA/Harbinger	chr4:2,076,980-2,077,351
AT4TE10335	ATCOPIA58	LTR/Copia	chr4:2,198,163-2,203,991
AT4TE15005	ATHILA3	LTR/Gypsy	chr4:3,266,370-3,288,501
AT4TE15025	ATHILA0_I	LTR/Gypsy	chr4:3,273,946-3,285,539
AT4TE15030	ATHILA6A	LTR/Gypsy	chr4:3,274,431-3,285,232
AT4TE16900	ATHILA	LTR/Gypsy	chr4:3,838,635-3,843,992
AT4TE17090	ATCOPIA41	LTR/Copia	chr4:3,909,249-3,910,990
AT4TE17115	ATHILA6A	LTR/Gypsy	chr4:3,915,207-3,916,819
AT4TE20120	ATENSPM5	DNA/En-Spm	chr4:4,830,277-4,836,762
AT4TE25590	ATCOPIA49	LTR/Copia	chr4:6,067,394-6,072,632
AT5TE35950	HELITRONY1D	RC/Helitron	chr5:9,871,833-9,872,483
AT5TE39170	ATGP1	LTR/Gypsy	chr5:10,764,247-10,772,507
AT5TE39630	ATIS112A	DNA/Harbinger	chr5:10,901,855-10,903,021

AT5TE43315	ATHILA	LTR/Gypsy	chr5:12,182,325-12,187,588
AT5TE46210	ATHILA8B	LTR/Gypsy	chr5:13,008,325-13,013,667
AT5TE47200	ATHILA2	LTR/Gypsy	chr5:13,334,474-13,345,770

PCGs upregulated in *in the atmorc1-3 atmorc6-1 double mutant*	
NAME	GENE ANNOTATION
AT3G20710	F-box protein-related
AT4G05370	unknown protein
AT3G13220	ABC transporter family protein
AT3G15440	unknown protein
AT3G22860	TIF3C2 (eukaryotic translation initiation factor 3 subunit C2)
AT5G29560	Ca+2-binding EF hand family protein
AT1G45063	copper ion binding / electron carrier
AT3G44460	DPBF2 (BASIC LEUCINE ZIPPER TRANSCRIPTION FACTOR 67)
AT3G30842	ATPDR10/PDR10 (PLEIOTROPIC DRUG RESISTANCE 10)
AT1G27570	phosphatidylinositol 3- and 4-kinase family protein
AT2G17690	F-box family protein
AT3G29639	unknown protein
AT2G04050	MATE efflux family protein
AT5G60260	unknown protein
AT4G05380	AAA-type ATPase family protein
AT1G33840	unknown protein
AT2G10975	unknown protein
AT5G18840	sugar transporter, putative
AT1G36675	glycine-rich protein
AT1G35730	APUM9 (ARABIDOPSIS PUMILIO 9); RNA binding (APUM9)
AT3G01345	unknown protein
AT1G15150	MATE efflux family protein
AT4G36850	PQ-loop repeat family protein / transmembrane family protein
AT1G27565	unknown protein
AT2G07213	other_rna
AT5G23020	MAM-L (METHYLTHIOALKYMALATE SYNTHASE-LIKE); 2-isopropylmalate synthase
AT5G45095	unknown protein
AT4G20820*	FAD-binding domain-containing protein
AT2G07215	unknown protein
AT3G14380	integral membrane family protein
AT3G47340	ASN1 (DARK INDUCIBLE 6)
AT5G07700*	MYB76 (myb domain protein 76); DNA binding / transcription factor
AT5G41080	glycerophosphoryl diester phosphodiesterase family protein
AT3G33528	unknown protein
AT3G09450	unknown protein
AT5G38386	F-box family protein
AT2G18193	AAA-type ATPase family protein
AT5G36910	THI2.2 (THIONIN 2.2); toxin receptor binding (THI2.2)
AT3G44990*	XTR8 (xyloglucan:xyloglucosyl transferase 8); hydrolase, acting on glycosyl bonds (XTR8)
AT3G01600	ANAC044 (Arabidopsis NAC domain containing protein 44); transcription factor
AT1G07450*	tropinone reductase, putative / tropine dehydrogenase, putative
AT4G15680	glutaredoxin family protein

Table S4: Sequences of primers used in this study		
T-DNA genotyping		
JP9339	atmorc6-3_LP	GGAAAGCTGGAAGCTATAATGATG
JP9340	atmorc6-3_RP	GATGACATCTGCCCCAAGTCTC
JP7707	GABI-KAT LB O8409	ATATTGACCATCATACTCATTGC
JP8938	atmorc1-4_LP	CGTATCTCAGCCGCTAACTTG
JP8939	atmorc1-4_RP	AAGCAGCTGCAGTGGATTATG
JP2207	LB3 SAIL T-DNA	TAGCATCTGAATTTCATAACCAATCTCGATACAC
JP8509	drm2-2_LP	AGATCGCTTCCAGAGTTAGCC
JP8510	drm2-2_RP	TTGTCGCAAAAAGCAAAAGAG
JP2922	cmt3-11_LP	TAACGGAAGGATGCCAGATT
JP2923	cmt3-11_RP	CAAGAAATGGGCTGTTGACAT
JP2410	LBA1 SALK T-DNA	TGGTTCACGTAGTGGGCCATCG
RT-qPCR		
JP2452	ACTIN 7_LP	TCGTGGTGGTGAGTTTGTTAC
JP2453	ACTIN 7_RP	CAGCATCATCACAAGCATCC
JP3395	SDC_LP	AATGTAAGTTGTAAACCATTTGAACGTGACC
JP3396	SDC_RP	CAGGCATCCGTAGAACTCATGAGC
JP9642	ROMANIAT5_LP	GTATCCTTTGGCCCGGTATT
JP9643	ROMANIAT5_RP	GCCTCTTCGAAATGCCATAA
JP9055	ATCOPIA28_LP	AGTCCTTTTGGTTGCTGAACA
JP9056	ATCOPIA28_RP	CCGGATGTAGCAACATTCACT
JP9640	soloLTR_LP	AACTAACGTCATTACATACACATCTTG
JP9641	soloLTR_RP	AATTAGGATCTTGTTTGCCAGCTA
JP9057	ATMU1_LP	TAATTTGGCTGACGGAATCAC
JP9058	ATMU1_RP	ATTTGGGGGAAAACAAATGAG
JP9646	atmorc6-3_LP	CATGTGCACCCTATGTTCCTT
JP9647	atmorc6-3_RP	ATCCCTTGGATTTGTGGTTTT
JP9680	atmorc1-4_LP	ATCAAGGAGGCCCCTAAACTT
JP9681	atmorc1-4_RP	TGTGACAGTGATTTTGCCAGT
BS-sequencing		
JP6349	SDC_BSPCR_LP	GAAAAAGTTGGAATGGGTTTGGAGAGTTTAA
JP6350	SDC_BSPCR_RP	CAACAAACCCTAATATATTTTATATTAAAAC
JP9775	ROMANIAT5_BSPCR_LP	GTAAGTGGATTAGTTATTAAAAGAGAGTT
JP9776	ROMANIAT5_BSPCR_RP	ATAAATAAACATCATCTACATCTTATAA
JP9120	ATCOPIA28_BSPCR_LP	TATTTATTTYGTTCATTTGGATTAGTTTT
JP9121	ATCOPIA28_BSPCR_RP	ACRATATCAAAATAATTATCATCATCTTAA
JP9377	soloLTR_BSPCR_LP	GATATAAAGGAATGGTTAGATAATATGYGATT
JP9378	soloLTR_BSPCR_RP	CRATATAACTCAAAATTTATATTACTCTTAA
JP9177	ATMU1_BSPCR_LP	TTATGAATTAGTTAGGTTATAGTTTGTTTATT
JP9178	ATMU1_BSPCR_RP	ATTCCTCRTCTTCTACAACATCATTTAA
Cloning		
JP5275	PstI_SDCpro_fwd	GTAACTGCAGTGATGCTCTAACAATTCTTTCCACAAGACC
JP5276	PstI_SDCpro_rev	GAAACTGCAGTTCTCTCCCCTGTTTTTGCTACTATTG
JP5235	HindIII-NLS-eGFP_FWD	TGGCAAGCTTATGGCTCCAAAGAAGAAGAGAAAGGTCATG
JP5236	HindIII_35Sterminator_REV	TAGCAAGCTTCTCTCAACACATGAGCGAAACCCTATAAG
JP8644	ATMORC1_Ctertag_LP	CACCGTTGATTTGGTTTTGTCTGGTC
JP8645	ATMORC1_Ctertag_RP	AACTTGTTGCATCTCCTTCTTC
JP8646	ATMORC6_Ctertag_LP	CACCAGTATGATGTGAGGTTAGTGAG

JP8647	ATMORC6_Ctertag_RP	CGTATTTACATTTCTTCTGTGC

References and Notes

1. J. A. Law, S. E. Jacobsen, Establishing, maintaining and modifying DNA methylation patterns in plants and animals. *Nat. Rev. Genet.* **11**, 204 (2010). doi:10.1038/nrg2719 Medline

2. J. P. Jackson, A. M. Lindroth, X. Cao, S. E. Jacobsen, Control of CpNpG DNA methylation by the KRYPTONITE histone H3 methyltransferase. *Nature* **416**, 556 (2002). doi:10.1038/nature731 Medline

3. F. Malagnac, L. Bartee, J. Bender, An Arabidopsis SET domain protein required for maintenance but not establishment of DNA methylation. *EMBO J.* **21**, 6842 (2002). doi:10.1093/emboj/cdf687 Medline

4. X. Zhang *et al*., Genome-wide high-resolution mapping and functional analysis of DNA methylation in arabidopsis. *Cell* **126**, 1189 (2006). doi:10.1016/j.cell.2006.08.003 Medline

5. I. R. Henderson, S. E. Jacobsen, Tandem repeats upstream of the Arabidopsis endogene SDC recruit non-CG DNA methylation and initiate siRNA spreading. *Genes Dev.* **22**, 1597 (2008). doi:10.1101/gad.1667808 Medline

6. H. G. Kang, J. C. Kuhl, P. Kachroo, D. F. Klessig, CRT1, an Arabidopsis ATPase that interacts with diverse resistance proteins and modulates disease resistance to turnip crinkle virus. *Cell Host Microbe* **3**, 48 (2008). doi:10.1016/j.chom.2007.11.006 Medline

7. H. G. Kang *et al*., Endosome-associated CRT1 functions early in resistance gene-mediated defense signaling in Arabidopsis and tobacco. *Plant Cell* **22**, 918 (2010). doi:10.1105/tpc.109.071662 Medline

8. Z. Wang, M. Gerstein, M. Snyder, RNA-Seq: a revolutionary tool for transcriptomics. *Nat. Rev. Genet.* **10**, 57 (2009). doi:10.1038/nrg2484 Medline

9. S. J. Cokus *et al*., Shotgun bisulphite sequencing of the Arabidopsis genome reveals DNA methylation patterning. *Nature* **452**, 215 (2008). doi:10.1038/nature06745 Medline

10. M. L. Watson *et al*., Identification of morc (microrchidia), a mutation that results in arrest of spermatogenesis at an early meiotic stage in the mouse. *Proc. Natl. Acad. Sci. U.S.A.* **95**, 14361 (1998). doi:10.1073/pnas.95.24.14361 Medline

11. N. Inoue *et al*., New gene family defined by MORC, a nuclear protein required for mouse spermatogenesis. *Hum. Mol. Genet.* **8**, 1201 (1999). doi:10.1093/hmg/8.7.1201 Medline

12. L. M. Iyer, S. Abhiman, L. Aravind, MutL homologs in restriction-modification systems and the origin of eukaryotic MORC ATPases. *Biol. Direct* **3**, 8 (2008). doi:10.1186/1745-6150-3-8 Medline

13. P. Fransz, J. H. De Jong, M. Lysak, M. R. Castiglione, I. Schubert, Interphase chromosomes in Arabidopsis are organized as well defined chromocenters from

which euchromatin loops emanate. *Proc. Natl. Acad. Sci. U.S.A.* **99**, 14584 (2002). doi:10.1073/pnas.212325299 Medline

14. E. Lieberman-Aiden *et al*., Comprehensive mapping of long-range interactions reveals folding principles of the human genome. *Science* **326**, 289 (2009). doi:10.1126/science.1181369 Medline

15. P. Amedeo, Y. Habu, K. Afsar, O. Mittelsten Scheid, J. Paszkowski, Disruption of the plant gene MOM releases transcriptional silencing of methylated genes. *Nature* **405**, 203 (2000). doi:10.1038/35012108 Medline

16. A. V. Probst, P. F. Fransz, J. Paszkowski, O. Mittelsten Scheid, Two means of transcriptional reactivation within heterochromatin. *Plant J.* **33**, 743 (2003). doi:10.1046/j.1365-313X.2003.01667.x Medline

17. V. J. Simpson, T. E. Johnson, R. F. Hammen, Caenorhabditis elegans DNA does not contain 5-methylcytosine at any time during development or aging. *Nucleic Acids Res.* **14**, 6711 (1986). doi:10.1093/nar/14.16.6711 Medline

18. S. Kennedy, D. Wang, G. Ruvkun, A conserved siRNA-degrading RNase negatively regulates RNA interference in C. elegans. *Nature* **427**, 645 (2004). doi:10.1038/nature02302 Medline

19. H. Tabara *et al*., The rde-1 gene, RNA interference, and transposon silencing in C. elegans. *Cell* **99**, 123 (1999). doi:10.1016/S0092-8674(00)81644-X Medline

20. M. A. Carmell *et al*., MIWI2 is essential for spermatogenesis and repression of transposons in the mouse male germline. *Dev. Cell* **12**, 503 (2007). doi:10.1016/j.devcel.2007.03.001 Medline

21. D. Bourc'his, T. H. Bestor, Meiotic catastrophe and retrotransposon reactivation in male germ cells lacking Dnmt3L. *Nature* **431**, 96 (2004). doi:10.1038/nature02886 Medline

22. A. A. Aravin *et al*., A piRNA pathway primed by individual transposons is linked to de novo DNA methylation in mice. *Mol. Cell* **31**, 785 (2008). doi:10.1016/j.molcel.2008.09.003 Medline

23. M. W. Kankel *et al*., Arabidopsis MET1 cytosine methyltransferase mutants. *Genetics* **163**, 1109 (2003). Medline

24. N. Kleinboelting, G. Huep, A. Kloetgen, P. Viehoever, B. Weisshaar, GABI-Kat SimpleSearch: new features of the Arabidopsis thaliana T-DNA mutant database. *Nucleic Acids Res.* **40**, (Database issue), D1211 (2012). doi:10.1093/nar/gkr1047 Medline

25. S. J. Clough, A. F. Bent, Floral dip: a simplified method for Agrobacterium-mediated transformation of Arabidopsis thaliana. *Plant J.* **16**, 735 (1998). doi:10.1046/j.1365-313x.1998.00343.x Medline

26. J. A. Law, A. A. Vashisht, J. A. Wohlschlegel, S. E. Jacobsen, SHH1, a homeodomain protein required for DNA methylation, as well as RDR2, RDM4, and chromatin remodeling factors, associate with RNA polymerase IV. *PLoS Genet.* **7**, e1002195 (2011). doi:10.1371/journal.pgen.1002195 Medline

27. M. V. Greenberg *et al*., Identification of genes required for de novo DNA methylation in Arabidopsis. *Epigenetics* **6**, 344 (2011). doi:10.4161/epi.6.3.14242 Medline

28. B. Langmead, C. Trapnell, M. Pop, S. L. Salzberg, Ultrafast and memory-efficient alignment of short DNA sequences to the human genome. *Genome Biol.* **10**, R25 (2009). doi:10.1186/gb-2009-10-3-r25 Medline

29. A. Mortazavi, B. A. Williams, K. McCue, L. Schaeffer, B. Wold, Mapping and quantifying mammalian transcriptomes by RNA-Seq. *Nat. Methods* **5**, 621 (2008). doi:10.1038/nmeth.1226 Medline

30. Y. Benjamini, Y. Hochberg, *J. R. Stat. Soc., B* **57**, 12 (1995).

31. P. Y. Chen, S. J. Cokus, M. Pellegrini, BS Seeker: precise mapping for bisulfite sequencing. *BMC Bioinformatics* **11**, 203 (2010). doi:10.1186/1471-2105-11-203 Medline

32. J. Lee *et al*., Analysis of transcription factor HY5 genomic binding sites revealed its hierarchical role in light regulation of development. *Plant Cell* **19**, 731 (2007). doi:10.1105/tpc.106.047688 Medline

33. C. Lu, B. C. Meyers, P. J. Green, Construction of small RNA cDNA libraries for deep sequencing. *Methods* **43**, 110 (2007). doi:10.1016/j.ymeth.2007.05.002 Medline

34. Y. Zhang *et al*., Spatial organization of the mouse genome and its role in recurrent chromosomal translocations. *Cell* **148**, 908 (2012). doi:10.1016/j.cell.2012.02.002 Medline

35. W. J. Soppe *et al*., DNA methylation controls histone H3 lysine 9 methylation and heterochromatin assembly in Arabidopsis. *EMBO J.* **21**, 6549 (2002). doi:10.1093/emboj/cdf657 Medline

36. J. K. Kim *et al*., Functional genomic analysis of RNA interference in C. elegans. *Science* **308**, 1164 (2005). doi:10.1126/science.1109267 Medline

37. R. S. Kamath *et al*., Systematic functional analysis of the Caenorhabditis elegans genome using RNAi. *Nature* **421**, 231 (2003). doi:10.1038/nature01278 Medline

38. Y. Y. Polosina, C. G. Cupples, Wot the ’L-Does MutL do? *Mutat. Res.* **705**, 228 (2010). doi:10.1016/j.mrrev.2010.07.002 Medline

39. Y. Mimura, K. Takahashi, K. Kawata, T. Akazawa, N. Inoue, Two-step colocalization of MORC3 with PML nuclear bodies. *J. Cell Sci.* **123**, 2014 (2010). doi:10.1242/jcs.063586 Medline

40. T. Hirano, The ABCs of SMC proteins: two-armed ATPases for chromosome condensation, cohesion, and repair. *Genes Dev.* **16**, 399 (2002). doi:10.1101/gad.955102 Medline

41. M. E. Blewitt *et al*., SmcHD1, containing a structural-maintenance-of-chromosomes hinge domain, has a critical role in X inactivation. *Nat. Genet.* **40**, 663 (2008). doi:10.1038/ng.142 Medline

42. I. Ausin, T. C. Mockler, J. Chory, S. E. Jacobsen, IDN1 and IDN2 are required for de novo DNA methylation in Arabidopsis thaliana. *Nat. Struct. Mol. Biol.* **16**, 1325 (2009). doi:10.1038/nsmb.1690 Medline

43. T. Kanno *et al*., A structural-maintenance-of-chromosomes hinge domain-containing protein is required for RNA-directed DNA methylation. *Nat. Genet.* **40**, 670 (2008). doi:10.1038/ng.119 Medline

44. G. Böhmdorfer *et al*., GMI1, a structural-maintenance-of-chromosomes-hinge domain-containing protein, is involved in somatic homologous recombination in Arabidopsis. *Plant J.* **67**, 420 (2011). doi:10.1111/j.1365-313X.2011.04604.x Medline